CONSIGLIO NAZIONALE DELLE RICERCHE

ISTITUTO DI SCIENZA E TECNOLOGIA DELL'INFORMAZIONE

LABORATORIO SEGNALI E IMMAGINI

Towards the Wize Sniffer 1.1 : A functional gas sensor for breath analysis

D. Germanese (ISTI- CNR)
M. Righi (ISTI- CNR)
M. D'Acunto (ISTI- CNR)
M. Magrini (ISTI- CNR)
P. Paradisi (ISTI- CNR)
M. Guidi (IGG- CNR)

TABLE OF CONTENT

ABBREVIATIONS AND ACRONYMS

KNN	K nearest voting rule
ml	milliliter
PCA	Principal Component Analysis
PANi	polyaniline
PEO	Polyethylene oxide
Ppm	parts per million
PPY	polypirrole
PPV	poly(p-phenylene vinylene)
SEM	Scanning Electron Microscope
WS	Wize Sniffer
VOC	Volatile Organic Compounds
ACDs	Atherosclerotic Cardiovascular Diseases
GC	Gas Chromatography
s	seconds
USB	Universal Serial Bus
RH	Relative Humidity
EMF	Electromotive Force
HME	Heat and Exchange Moisturizers
PWM	Pulse With Modulation
ISO/OSI	Open System Interconnection/International Organization for Standardization
TCP	Transmission Control Protocol
IP	Internet Protocol
MAC	Media Access Control
BAC	Blood Alcohol Concentration
BrAC	Breath Alcohol Concentration
ABS	Acrylonitrile butadiene styrene
SRAM	Static Random Access Memory

TABLE OF FIGURES

TABLE LEGENDS

EXECUTIVE SUMMARY

In this report, we describe the manufacturing of a device for breath analysis. Breath analysis offers a relatively inexpensive, rapid, and non-invasive method for detecting a variety of life habits and possible diseases. Our activity was focused on the design and functionality of the Wize Sniffer (WS), a new portable device for breath analysis limited to an effective number of substances. Within the European SEMEOTICONS (SEMEiotic Oriented Technology for Idividual's CardiOmetabolic risk self-assessmeNt and Self-monitoring) Project by the WS, we intend a hardware/software tool for both the analysis of volatile organic compounds of breath and a platform for data mining and data integration. The WS should be able to provide useful information about the "breathprint", i.e., the analog of fingerprint for the state of health of an individual, to be used in the Virtual Individual Map.

In this first period of activity, the WS has been designed in two main configurations. One configuration to work with commercial sensors (that is going to be operative) and the other one configuration to work with customized sensors made using electrospun nanofibers as sensing material. This last configuration is still work in progress.

The efforts for the design of the WS involved also statistical data processing.

1. PURPOSE AND SCOPE OF THIS DOCUMENT

The report will focus on:

- The design and functionality of a portable device for breath analysis;
- The description of the volatile breath substances to be detected, and their link to the noxious habits for cardio-metabolic risk;
- The gas sensors to be used, both commercial sensors or improved new sensing devices employing conductive polymers;
- The accuracy of data processing.

In addition, anticipating some efforts already provided in the next deliverable, we describe the design and integration of the WS with communication architecture of the Wize Mirror, the multisensory platform (having the appearance of a mirror) which SEMEOTICONS aims to develop.

Breath gases are recognized to be excellent indicators of the presence of diseases and clinical conditions. Currently, such gases have been identified as biomarkers using very accurate but expensive, time consuming and non-portable instrumentations.

Essentially, a design of a portable device for breath analysis, such as WS, is based on selected chemical sensors that are sensitive to the biomarkers and compounds in breath substances and make use of accurate statistical tools for odor signal preprocessing, classification methods and, in turn, identification of possible diseases if any. The device captures breath samples, the chemical selective sensors sense the sample and accordingly form a sort of *odorprint* of healthy people or patients with known and specific diseases, in order to evaluate the *well-being* state of a human subject.

In this document, we describe all the different efforts required to design the portable WS.

2. INTRODUCTION

Atherosclerotic cardiovascular diseases (ACDs) represent the leading cause of worldwide mortality [1-2]. Breath gases are recognized to be excellent indicators of the presence of diseases and clinical conditions. Such gases have been identified as biomarkers using instrumentations such as gas chromatography (GC) or electronic nose (e-nose) [3]. GC is very accurate but expensive, time consuming and non portable. E-nose has the advantages of low-cost and easy operation, but is not particularly useful for analyzing breath substances. As a consequence, in recent years, it has been stimulated the necessity to develop a portable device for breath analysis, easy to use, and feasible for patients living far from medical structures or physicians.

Essentially, a design of a portable device for breath analysis is based on selected chemical sensors that are sensitive to the biomarkers and compounds in breath substances and make use of accurate statistical tools for odor signal preprocessing, classification methods and, in turn, identification of possible diseases if any. In SEMEOTICONS activity, we are developing a device following the above requirement. The device, called Wize Sniffer (WS), captures breath samples, the chemical selective sensors sense the sample and accordingly form a sort of *odorprint* of healthy people or patients with known and specific diseases, in order to evaluate the *well-being* state of a human subject [4]. It should be noted that does not exist a general definition of "well-being state", rather some indices for well-being that can be correlated to cardio-metabolic risk. In addition, such indices are strictly connected to the recognition of behavioral trends and the methods for computing the raw numerical values of such well-being indices must be designed for single individual. However, one critical index of well-being is given by the breath composition. Human breath is largely composed of oxygen, carbon dioxide, water vapor, nitric oxide, and numerous volatile organic compounds (VOCs) [5-6]. The type and number of VOCs in the breath changes among different individuals, but there is a common core of breath VOCs which are present in all individuals. The molecules in an individual's breath may be exogenous or endogenous. Exogenous molecules are those that have inhaled or ingested from the environment or other sources such as air or food, thus giving no diagnostic value. Endogenous molecules are produced by metabolic processes and partition from blood via the alveolar pulmonary membrane into the alveolar air. Such endogenous molecules are present in breath relatively to their types, concentrations, volatilities, lipid solubility and rates of diffusion as they circulate in the blood and cross the alveolar membrane. Changes in the concentration of the molecules in VOCs could suggest various diseases or at least changes in the metabolism.

In this report, we present the design of a portable device able to operate with a limited number of breath VOCs, normally connected to oxidative stress, thus giving information to physicians on the possible state of wellness of an individual.

2.1 BREATH ANALYSIS AND WELL-BEING STATES

Breath analysis, as performed by our portable device, is done with a limited number of breath VOCs, normally connected to oxidative stress, thus giving information to physicians on the possible state of wellness of an individual. Oxidative stress describes an imbalance between the systemic manifestation of reactive oxygen species and the ability of a biological system to readily detoxify the reactive intermediates or to repair the resulting damage. So a direct connection between oxidative stress and well-being state is immediate.

The most relevant VOCs and their correlation to oxidative stress and considered for the design of the WS are labelled as follows.

Carbon Monoxide (CO): it is naturally produced by the action of heme oxygenase on the heme for haemoglobin breakdown. This produces carboxyhemoglobin, which is a more stable molecule than oxyhemoglobin. For example, an increase of CO leads haemoglobin to carry less oxygen through the vessels. CO is present in cigarette smoke (it is the major component, (75,95%) and air pollution too. In addition, it is a blood vessel relaxant (vasodilator), and a promoter of neurovascular growth (it's not always beneficial, since it plays a bad role in tumor growth). Mean carbon monoxide concentration in exhaled breath is about 3,5 ppm. Increasing levels of exhaled carbon monoxide can be detected in smoking subjects: 13.8 - 29 ppm.

Because of these carbon monoxide's roles in the body, abnormalities in its metabolism have been linked to a variety of diseases, including neurodegenerations, hypertension, heart failure, and inflammation.

Carbon Dioxide (CO_2): Mean carbon dioxide concentration in exhaled breath is about 4% (= 40000ppm). It is produced as a waste product when energy is released during certain metabolic reactions of cellular respiration.

In healthy individuals, partial pressure in arterial blood is very close to the partial pressure in expired gases. So, carbon dioxide production can be considered as a measure of metabolism. Not only, it can be considered a good index for oxidative stress. Indeed, among all the reactions present within cellular respiration there is the oxidative phosphorylation that produces not only carbon dioxide, but also reactive oxygen species such as superoxide and hydrogen peroxide. This lead to propagation of free radicals, which can damage cells and contribute to the onset of many disease. The increase of CO2 can be due also to physical activity, for example. There is a decrease in presence of some forms of congenital heart disease (for example, cyanotic lesions that result in a bluish-grey discoloration of the skin and in a lack of O2 in the body). Also individual's breathing rate influences the level of CO2 in blood and, as a consequence, in exhaled gas. Breathing that is too slow causes respiratory acidosis (that results in an increase of CO2 partial pressure in blood, which may cause hypertension, build up of heart rate), while breathing that is too rapid leads to hyperventilation, which may cause respiratory alkalosis (that results in decrease of CO2 in blood; so, it can no longer fulfill its role of vasodilator, resulting in arrhythmias, extra systoles). Carbon dioxide is also one of constituents of tobacco smoke (it is present in 13%).

Ethanol: the ethanol component in a breath composition can be classified as endogenous or exogenous. Endogenous Ethanol (whose values are very low: 0.62ppm) may increase in exhaled gas mixtures because of alcoholic fermentation of an excessive over-load of carbohydrates. Indeed it is originated from microbial fermentation of carbohydrates in the gastro-intestinal tract. Then, it enters in the blood. On the contrary, exogenous Ethanol comes from alcoholic drink. It is important to note that it is recognized that ethanol breakdown leads to an accumulation of free radicals into the cells, a clear example of oxidative stress. Ethanol may cause arrhythmias and depresses the contractility of cardiac muscle.

Nitrogen Oxide (NO): it is a vasodilator and it modulates inflammatory response (operating in combination with CO and Hydrogen Sulfide). It is also a good indicator for asthma diseases. It is present in tobacco fumes, too.

Hydrogen Sulfide (H_2S): it is a vascular relaxant agent, and has a therapeutic effect in various cardiovascular diseases (myocardial injury, hypertension). In general, H_2S could have therapeutic effect against oxidative stress due to its capability to neutralize the action of free radicals. In patients with coronary heart disease, H_2S level in blood is normally reduced, as in the case of hypertension. On the contrary, in haemorrhagic shock, H_2S plasma levels are increased.

Ammonia (NH_3): Mean baseline levels of ammonia in exhaled gas are about 0.42ppm. Elevated breath ammonia usually could be due to liver disease, such also to kidney disease.

Nevertheless, ammonia is also one of the three major compounds, together with nitric oxide and carbon monoxide, of tobacco fumes (it is present in approximately 22,15%). All these three gases can have detrimental effects on the respiratory system. About ammonia, it forms a strong alkaline solution with water. When inhaled, ammonia irritates the upper respiratory tract including the nasal cavity, pharynx, larynx and trachea. Irritation results in coughing and hoarseness.

Hydrogen: The passage of unabsorbed dietary carbohydrate into the caecum is followed in most individuals by the production of hydrogen, a metabolic consequence of carbohydrate fermentation by anaerobic bacteria. This hydrogen traverses the gut wall, and is transported via the circulation to the lungs, where is execrated in exhaled breath.

Not only, a certain amount of exhaled hydrogen is the result of fermentation by oropharingeal bacteria. As a consequence, increased values of breath hydrogen may be due to overweight problems, intestinal diseases, improper life-style. A rise in exhaled hydrogen values occurs while/after smoking. A decrease occurs after exercise and in case of hyperventilation, which reduce the concentration of exhaled breath hydrogen by ”washing out” it from the lungs. About the quantities, for hydrogen the baseline value is about 9.1ppm.

Oxygen: Exhaled air has a decreased amount of oxygen and an increased amount of carbon dioxide. These amounts show how much oxygen is retained within the body for use by the cells and how much carbon dioxide is produced as a by-product of cellular metabolism.

Exhaled oxygen amount is about 13.6%-16%. Lower values may be due to respiration disorders. Not only, it is well known that, in smokers, carbon monoxide molecules take the place of oxygen in red blood cells, reducing the amounts of oxygen in blood and in exhaled gas.

Cigarette smoke: it contains principally Nicotine, CO, NH_3, oxidant substances leading to oxidative stress. After 1 minute smoking, an increase of heart rate can be revealed. Tobacco combustion causes a constriction of blood vessels.

Other factors leading to oxidative stress are cholesterol and fibrinogen. An increase of cholesterol leads to atherosclerotic issues and, similarly, an increase of fibrinogen leads to blood viscosity. In addition, a strong correlation exists between exhaled hydrocarbons and cardiovascular diseases, principally pentane and ethane. In healthy subjects, there is a balance between oxidant molecules (free radicals) and anti-oxidant molecules. When free radicals are balanced, they have a positive effect on the general person wellness and health, because they are involved in many inflammatory processes, thus having a therapeutic potential. On the contrary, when free radicals number exceeds the anti-oxidant ones, this leads to oxidative stress.

3. WIZE SNIFFER: DESIGN AND FUNCTIONALITY. AN OVERVIEW

The WS has been designed to be able to detect some breath compounds associated to cardio-metabolic risk factors. To this end, we will combine largely employed commercial chemical gas sensors with a new system of breath sensors made of electrospun nanofibers, in particular polianyline, polypirrole, etc.
The general idea of it has come from the study conducted by Dongmin Guo et al. [3], where a system like the one shown in Fig.1 is described.
The Wize Sniffer system operates in three phases: gas collection, gas sampling, and data analysis. It has a gas sampling bag/box (store chamber), an element (humidity filter) whose task is to absorb the water vapor from the breath, and a disposable mouthpiece. The gas sensors placed in the store chamber sense gas particles and generate measurable electronic signals, subsequently sent to the computer for feature extraction, pattern analysis and classification.
Temperature and humidity percentage will be measured in situ in the store chamber.

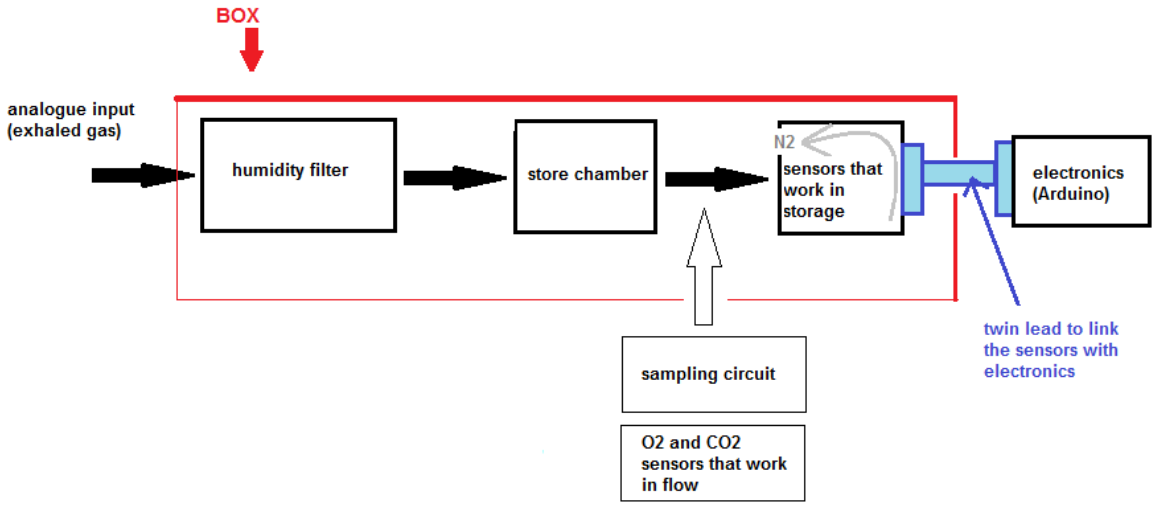

Fig.1. Schematic sketch of the WS system.

Sampling Procedure: The sampling procedure involves two sub-procedures, a purge cycle and a sampling cycle. In the purge cycle, a pump pulls and purges the air over the sensor array, supplying background air to the array for the baseline measurement as well as refreshing it after sampling. In the sample cycle, the analyte is injected into the accumulation chamber. When the sensor array is exposed to the analyte, changes in resistances are measured and recorded. The action of the system is different in each time-slice as detailed below:
1) -10 ~0*s* (baseline stage): The chamber is purged and the sensor returns to a steady state. The baseline value is measured and recorded for data manipulation and normalization;
2) 1 ~ 5*s* or 1~ 10*s* (injection stage): Sampled gas is injected into the chamber at an invariable rate. Particles of sampled gas inside the chamber accrue during injection, producing a changing of resistance of the sensor and causing the amplitude of the signal to rise;
3) 6(10) ~15*s* (reaction stage): Particles in the chamber continue to accumulate on the sensors, but the accumulation rate is decreasing. The resistance of the sensor monotonically increases at a decreasing rate, as does the amplitude of the signals;

4) 15~90*s* (purge stage): The chamber is purged again. The pump quickly draws out the remaining analyte, thereby, shortening the sampling time as well as refreshing the air for the next use.

In our database, the characteristic curve of one sample is taken from the data for the period from 1 s to 90s.

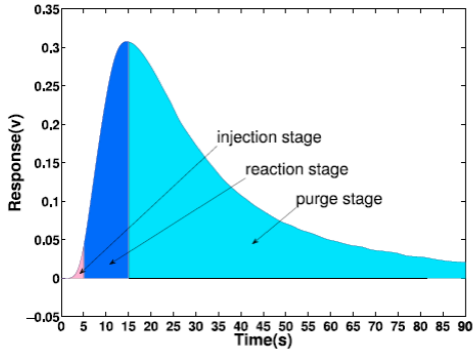

Fig. 2. A typical sensor response curve displaying the three stages. Note that the starting time for the reaction stage can fall in a 1-10 s varying range.

3.1 ELECTRSOPUN NANOFIBERS AS SENSING MATERIAL

The sensitivity of commercial sensors, as well as selectivity, can be improved reducing the sensing area. This achievement can be obtained using as sensing material conductive polymers electrospun nanofibers, (see Figure 3).

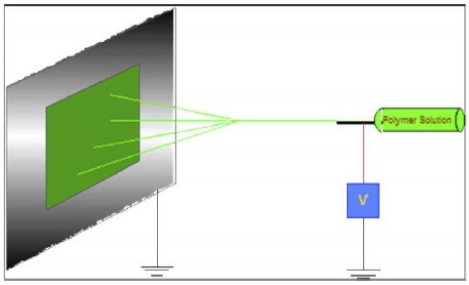

Fig. 3. A schematic sketch of electrospinning process.

Electrospinning is a manufacturing process able to produce ultra-fine fibers with diameters ranging from 50-500nm [8-9]. In the electrospinning process an electric field is generated between a polymer solution and a metal collection screen (collector). The polymer solution is contained in a syringe with a steel capillary tip and a voltage is applied between the tip and the conductive collector. As the electrical potential is increased, the charged polymer solution is attracted to the collector. When the voltage reaches a critical value, the charge overcomes the surface tension of the polymer solution formed on the capillary tip and an electrified jet is produced. As the charged jet flies through the air, it loses the solvent through a quick evaporation and impinges on the collection screen as a thin fiber mat. In the development of the WS, we will use electrospun nanofibers as sensing material and conductive polymers, such as polyaniline (PANi), polypirrole (PPY), poly(p-phenylene vinylene) (PPV) and others to be defined yet [10-12]. The advantage of sensors using nanofibers as sensing material would be a general increment of sensitivity and a significant reduction of the response time. Nevertheless, such properties must be evaluated during the measurement stages, and the possible response of such sensors is beyond the scope of the present paper.

3.2 STATISTICAL DATA PROCESSING

Since the operability of WS works on a *reduced space* of breath substances, data analysis requires a particular care because of the various sources of errors. The sensors measure changes in voltage across each sensor and convert the raw signal into a digital value that can be managed by physicians. Our analysis of sensor data requires three steps: signal preprocessing, feature extraction and classification. The aim of signal preprocessing is to compensate drifts and to eliminate irrelevant information so to improve the performance of the subsequent pattern recognition and classification. It is assumed that the dynamic response of any sensors is sampled introducing reasonable time intervals in a particular way for the transient phase. In addition, normalization is used to compensate for sample-to-sample variations caused by analyte concentrations and pressure of oxygen. At this point, we will introduce feature extraction from any sample using the standard procedure of principal component analysis (PCA) and, finally, *k*-nearest neighbor voting rule (KNN) will be used as a classifier for the features that extracted by PCA, [3].

4. THE FIRST WS: WIZE SNIFFER 1.0. BASIC SYSTEM FUNCTIONALITY OF WS 1.0

Since the WS device will be subject to different modifications in order to improve or to customize its functionality, we prefer to name the WS device with number progression used as follows: WS 1.x denote the version using the commercial sensors (for example, the current version using the commercial sensors, and going to be operative, is the WS 1.0), the WS version that will be designed with customized nanofibers-based sensors will be named WS 2.x.

The framework of all the WS devices (both 1.x or 2.x) consists of three modules: signal measurement, signal conditioning and signal acquisition. The total scheme of any WS device is sketched in figure 4:

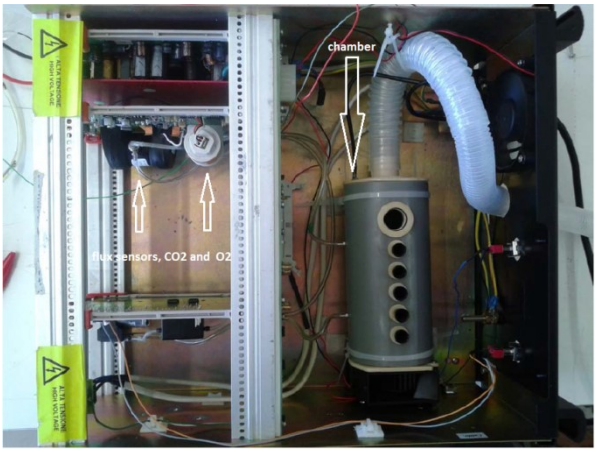

Fig. 4. A current configuration of the prototype WS 1.0

The device is composed as follows. The white arrows on the left denote, respectively, the CO2 and O2 sensors operating in flux mode making use of a sampling pump, and the chamber operating in gas accumulation, on right. The holes on the chamber quarter the commercial sensors.

The array of sensors is contained in the signal measurement module. The measurement circuit is responsible for transforming gas signals into electronic signals. The array sensors are mounted directly or connected with a griddle to a microcontroller board that can operate on the data collected filtering and amplifying them. The microcontroller used in our system is a widely employed open source controller: Arduino system that can be powered very simply via a USB connection.

4.1 THE COMMERCIAL GAS SENSORS

The choice of gas sensors has been made taking into account:

- The breath compounds to detect;
- The working principle of the sensors.

The aim of WS is to detect those compounds, present in human exhaled gas, that correlate with cardio-metabolic risk. As a consequence, our interest, during a first phase of the work, was focused on: **oxygen, carbon dioxide, carbon monoxide, ammonia, hydrogen, hydrocarbons, ethanol, hydrogen sulfide,** also according to the suggestions by SEMEOTICONS' physicians.

In a subsequent step, our efforts will be addressed to the development of PANI nanoyfiber-based gas sensors in order to detect substances such as **nitrogen oxide and nicotine**.

Criteria for choosing sensors' working principle, was based on their ease of use. So, we selected metal oxide semiconductor gas sensors. Their functioning is based on a variation of resistance from R_0 to Rs when the

sensor senses the gas particles. An analogue voltage is measured as indirect measure of change in resistance.
Furthermore, basing on the study of Guo et al. [3], we chose chemical gas sensors manufactured by Figaro Engineering, because such kind of sensors are very robust, sensitive, resistant to humidity and ageing.
We selected the following 6 gas sensors:

- **TGS 2602**: sensitive to hydrogen, ammonia, ethanol, hydrogen sulfide, toluene, cigarette smoke;
- **TGS 2620**: sensitive to hydrogen, carbon monoxide, ethanol, methane, isobutane;

These two sensors are "multi-substance", it means, they are not selective for one compound only, but they are able to detect more molecules at the same time.
The general sensors' structure is shown in Figure 5.

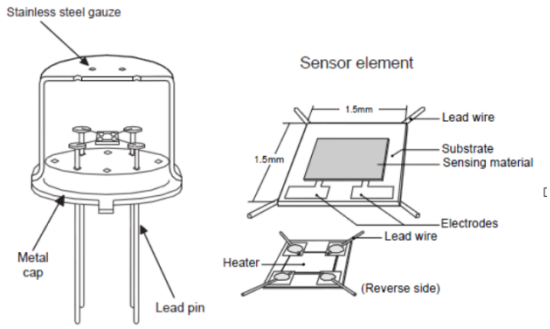

Fig. 5. Basic scheme of the metal oxide semiconductor sensors provided by Figaro Engineering.

Using thick film techniques, the sensor material is printed on electrodes (noble metal) which have been printed onto an alumina substrate. The main sensing material of the sensor element is metal oxide semiconductor.
One electrode is connected to pin No.2 and the other is connected to pin No.3 (see also Figure 6). A metal oxide heater printed onto the reverse side of the substrate and connected to pins No.1 and No.4 heats the sensing material, in order to maintain the sensor at a fixed temperature. Lead wires are Pt-W and are connected to sensor pins which are made of Ni-plated Ni-Fe 50%. The sensor base is made of Ni-plated steel. The sensor cap is made of stainless steel (SUS304).

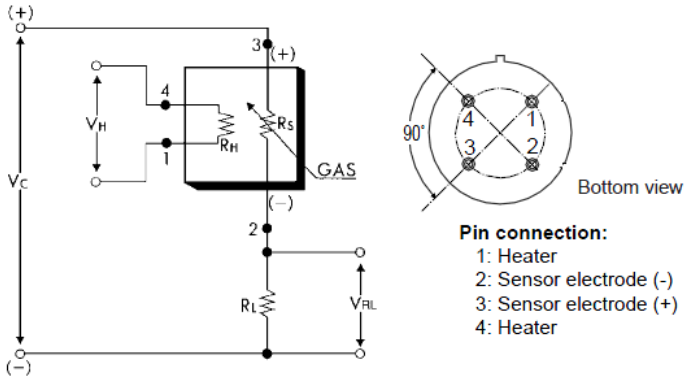

Fig. 6. The inner electrical circuit.

Fig.6 shows the basic measuring circuit, that is the same for TGS2602 and TGS2620.

A voltage (5V DC) is applied across the sensor element which has a resistance (Rs) between the sensor's two electrodes and the load resistor (RL) connected in series.
The sensor signal (VRL) is measured indirectly as a change in voltage across the RL. The Rs is obtained from the formula

$$Rs = \frac{Vc - VRL}{VRL} \times RL \qquad (1)$$

Figures 7 and 8 show, respectively, the sensitivity characteristics of the sensors TGS2620 and TGS2602 to various gases. Moreover, it is shown typical temperature and humidity dependency characteristics, too.

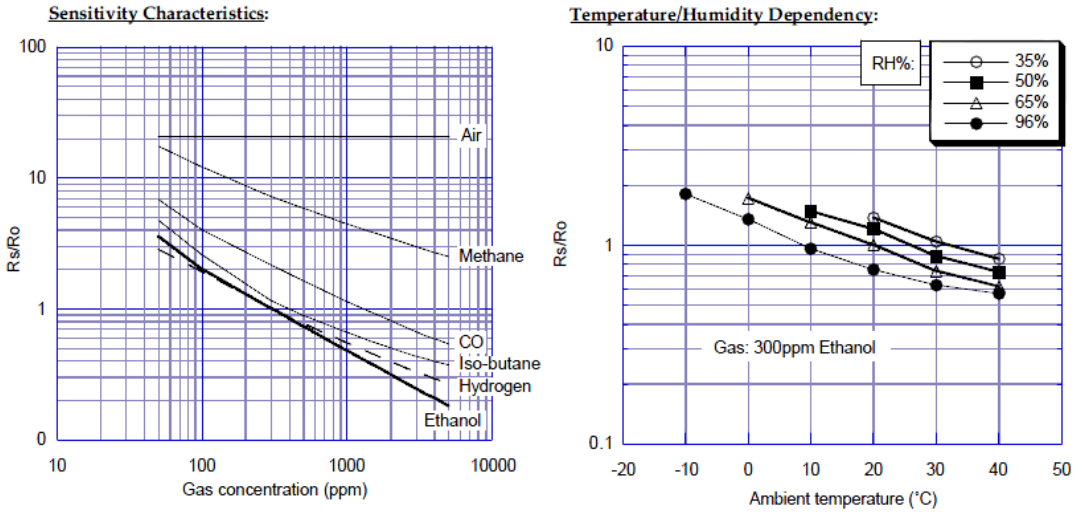

Fig. 7- TGS 2620- On the left, the Y-axis is indicated as sensor resistance ratio between Rs (= Sensor resistance in displayed gases at various concentrations) and Ro (= Sensor resistance in 300ppm of ethanol). On the right, the Y-axis is indicated as sensor resistance ratio between Rs (= Sensor resistance in 300ppm of ethanol at various temperature/humidity) and Ro (= Sensor resistance in 300ppm of ethanol taken at standard test conditions (20°C and 65%RH)).

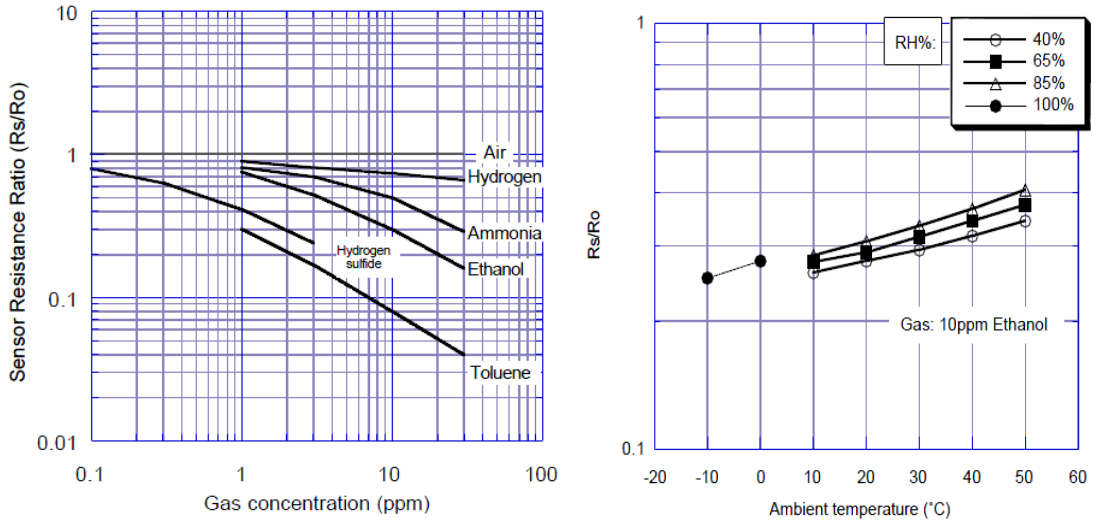

Fig. 8- TGS2602- On the left, the Y-axis shows the ratio of the sensor resistance in various gases (Rs) to the sensor resistance in clean air (Ro) taken at standard test conditions (20°C and 65%RH). On the right, The Y-axis shows the ratio of sensor resistance in 10ppm of ethanol under various atmospheric conditions (Rs) to the sensor resistance in clean air under the same atmospheric conditions (Ro).

In both cases, note that in the presence of a detectable gas, the sensor's conductivity increases depending on the gas concentration in the air. The temperature and humidity dependency characteristics prove that sensors' response depending on temperature and humidity. A heater circuit (see Fig.9) is provided, in order to maintain the sensor at a constant temperature.

➢ **TGS 4161**: sensitive to carbon dioxide;

It is a solid electrolyte CO2 sensor. By monitoring the change in electromotive force (EMF) generated between the two electrodes, it is possible to measure CO2 gas concentration.

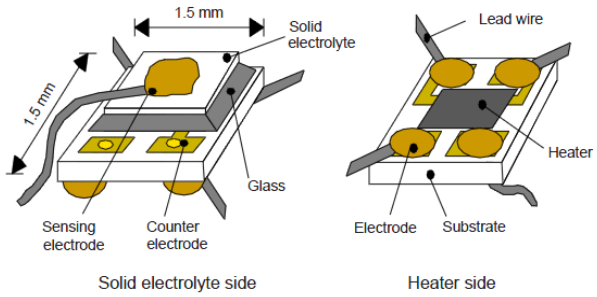

Fig. 9. The scheme of the electrolyte sensor TGS4161 from Figaro Engineering.

Figure 10 shows on the left the typical sensitivity characteristic (on a logarithmic scale) to carbon dioxide and on the right the humidity dependence.

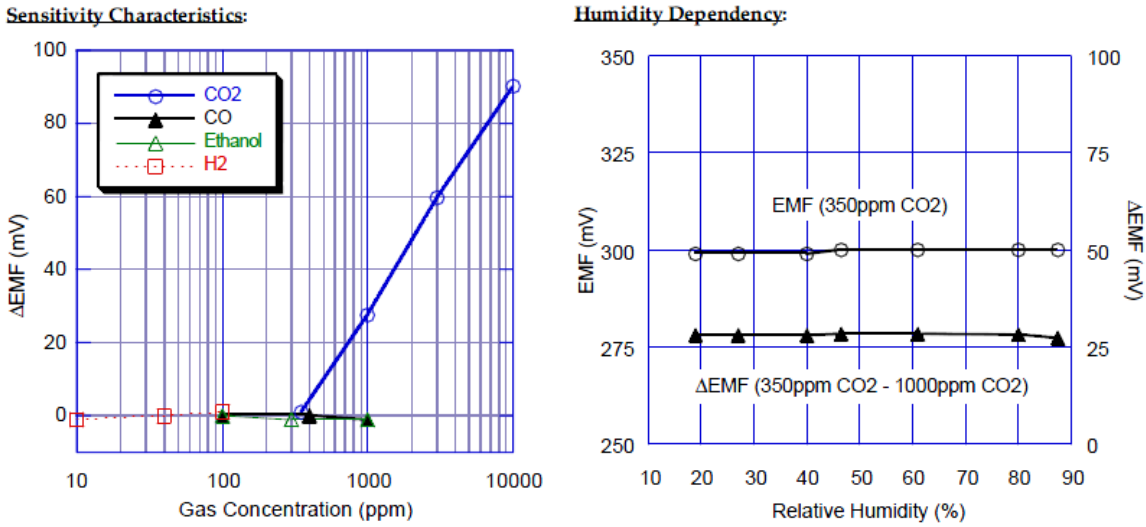

Fig. 10- On the left, the Y-axis shows Δ EMF which is defined as the difference between EMF1 and EMF2, where EMF1 equals EMF in 350 ppm CO2 and EMF2 equals EMF in listed gas concentration. On the right, the Y-axis shows Δ EMF which is defined as the difference between EMF1 and EMF2, where EMF1 equals EMF in 350 ppm CO2 and EMF2 equals EMF in 1000 ppm CO2. Note that the sensor shows a linear relationship, on logarithmic scale, between Δ EMF and carbon dioxide concentration. The sensor has also an excellent durability against high humidity effects.

In order to obtain an accurate measurement of CO2, it was integrated a special microprocessor for signal processing provided for TGS4161. Figaro Engineering makes available a special evaluation sensor module for this gas sensor: AM-4-4161 (shown in Figure 11).

Fig. 11. Electronic module for this gas sensor: AM-4-4161 from Figaro Engineering.

- **TGS 2442**: sensitive to carbon monoxide (shown in Fig.11, left);
- **TGS 2444**: sensitive to ammonia (shown in Fig.11, right);

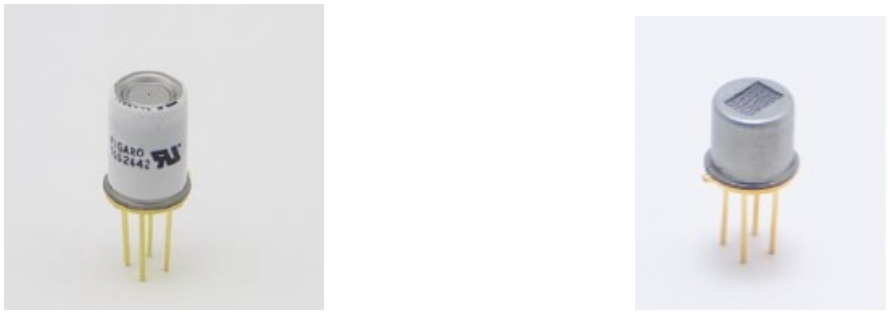

Fig. 12. The sensor TGS 24242, left and TGS 2444, right. Both from Figaro Engineering

Figures 13 and 14 show the sensitivity characteristics of these sensors (in addition, for TGS2442 is reported temperature and humidity dependence).

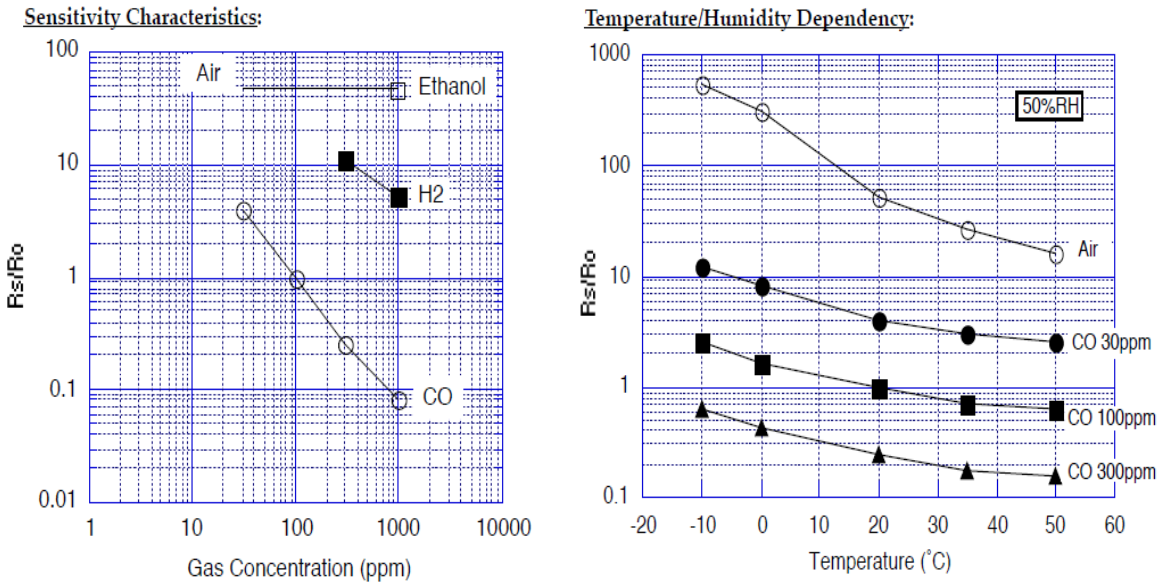

Figure 13 – TGS2442- On the left, the Y-axis shows the sensor's resistance ratio between Rs (= Sensor resistance of displayed gases at various concentrations) and Ro (= Sensor resistance in 100ppm CO). On the right, the Y-axis displays the sensor's resistance ratio between Rs (= Sensor resistance at 30ppm, 100ppm and 300ppm of CO at various temperatures and 50%RH) and Ro (= Sensor resistance at 300ppm of CO at 25°C and 50% RH).

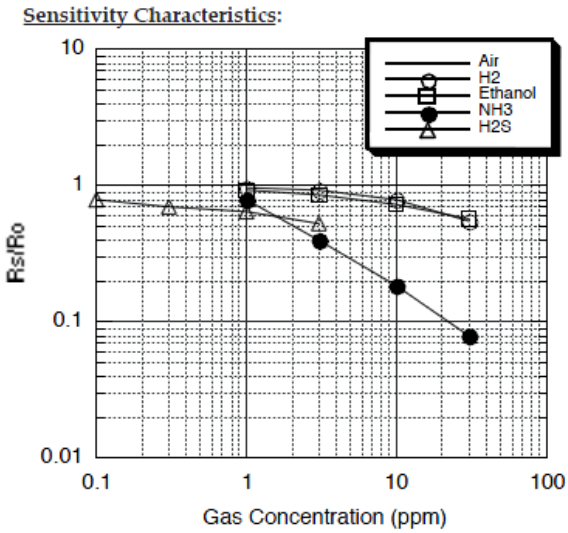

Fig. 14 – Sensor TGS2444. The Y-axis shows the sensor's resistance ratio between Rs (= Sensor resistance of displayed gases at various concentrations) and Ro (= Sensor resistance in air).

These two sensors require a basic measuring circuit like the one shown in Figure 15, left. Sensor's resistance is calculated as for TGS2602 and TGS2620, it means, by a voltage divider.

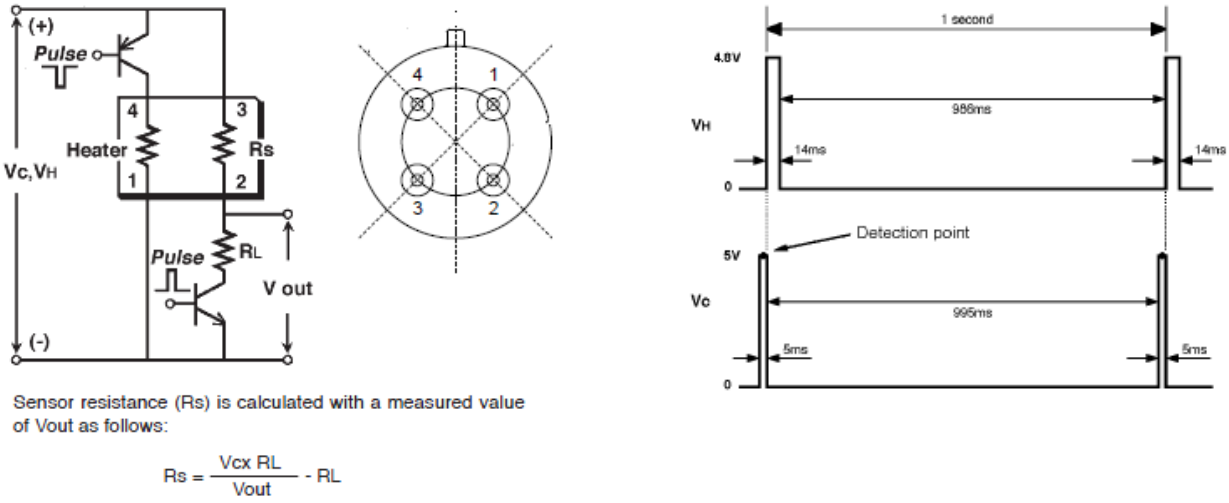

Sensor resistance (Rs) is calculated with a measured value of Vout as follows:

$$Rs = \frac{Vcx\ RL}{Vout} - RL$$

Fig. 15. Left, Basic measuring circuit for the sensors TGS2602 and TGS2620; right, the heating/powering cycle requested for TGS2442.

Application of a Vc pulse condition is required for TGS2442 to prevent possible migration of heater materials into the sensing element material. Under extreme conditions of high humidity and temperature, a constant Vc condition could result in such migration and cause long term drift of Rs to higher values.
A Vc pulse results in significantly less driving force for migration than a constant Vc condition, rendering the possibility of migration negligibly small.
For TGS2442 the heating/Vc cycle is shown in Figure 15, right.

- **TGS 821**: sensitive to hydrogen.

This metal oxide semiconductor sensor has the same behavior of TGS2602 and TGS2620.

The TGS821 sensitivity characteristics and temperature/humidity dependence are shown in Figure 16. As for the others sensors, the conductivity depends on the gas concentration.

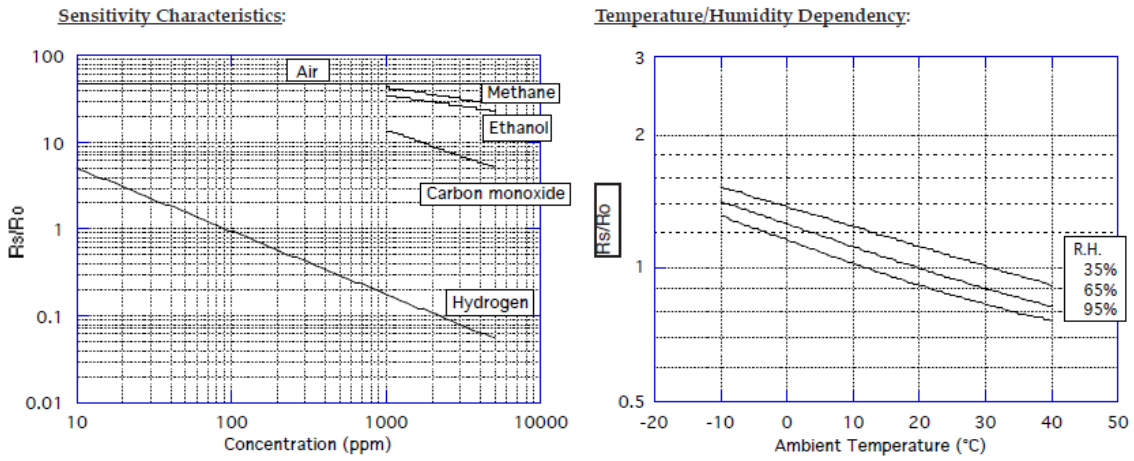

Fig. 16. On the left, Y-axis shows the resistance ratio between Rs (= Sensor resistance of displayed gases at various concentrations) and Ro (= Sensor resistance at 100ppm of hydrogen). On the right, Y-axis shows the resistance ratio between Rs (= Sensor resistance at 100ppm of hydrogen at various temperatures/humidities) and Ro (= Sensor resistance at 100ppm of hydrogen at 20°C and 65% R.H.).
The response times of all these sensors manufactured by Figaro Engineering are lower than 20-30sec.

4.2 TEMPERATURE AND HUMIDITY SENSORS

As described before, the sensitivity characteristic of each sensor varies according to humidity percentage present in the chamber or, generally, in the environment where the sensors are placed. That is the basic motivation we have considered appropriate to insert in the store chamber a temperature and humidity sensor. For this purpose, a Sensirion SHT11 (Figure 17, left) has been chosen.
It has been placed in the immediately chamber's entrance, as shown in Figure 17, right.

Fig.17. Sensirion SHT11 temperature sensor, left, and its location inside the store chamber, right.

Sensirion SHT11 has a humidity accuracy of about +/-3.5% and a temperature accuracy of about +/-0.5°C@25°C. It has a digital output, in contrast to other sensors (the gas ones) which have an analogue output.

4.3 COSMED GAS SENSORS

Two additional sensors, manufactured by COSMED s.r.l., one sensitive to **oxygen**, one sensitive to **carbon dioxide**, has been inserted in our device. These sensors work in *flowing-regime*: they sense gases' stream that is injected at a constant rate (120ml/sec) by the sampling pump. This electro-mechanic pump takes gas samples from the store chamber, injects them where the O2 and CO2 sensors are placed. Then, gases are brought back to store chamber.

About oxygen and carbon dioxide sensors' outputs, COSMED s.r.l. reported us the following informations:

- Warm-up time: 30min (for both sensors)
- Oxygen sensor's output: from 0 to 4V+/-0.01V @20.93% O2
- Carbon dioxide sensor's output:

0.02V +/-0.01V @ 0.03%
0.67V +/-0.01V @ 0.70%
1.75V +/-0.01V @ 2.00%
3.5V +/-0.01V @ 5.00%

Here, a table that summarizes the commercial sensors used in this first phase and molecules to be detected (Table 1).

Table 1. Sensors, detected molecules and optimal detection range.

SENSOR	DETECTED MOLECULE(S) / PHYSICAL QUANTITY	OPTIMAL DETECTION RANGE
FIGARO TGS2602	hydrogen, ammonia, ethanol, hydrogen sulfide	1-10 ppm
FIGARO TGS821	hydrogen	1-1000 ppm
FIGARO TGS2620	hydrogen, carbon monoxide, ethanol	50-5000 ppm
FIGARO TGS2442	ammonia	10-1000ppm
FIGARO TGS2444	carbon monoxide	10-100ppm
FIGARO TGS4161	carbon dioxide	350-10000ppm
COSMED	carbon dioxide	0%-5%
COSMED	oxygen	20.93%+/-10%
SENSIRION SHT11	temperature and humidity	-40°C-123°C 0%-100%

4.4 WIZE SNIFFER 1.0 FINAL SET-UP

Based on the block scheme in Fig.1, the individual breaths in a disposable mouthpiece placed at the tube's start. A heat and exchange moisturizers (HME) filter retains part of the humidity present in human exhaled breath. We provided for a corrugated tube (Figure 18A), necessary to convey the exhaled gas toward the store chamber where the six gas sensors (the commercial ones, manufactured by Figaro Engineering and described in precious section) are placed. Two uni-directional valves allow the gases to enter the chamber and to be collected within it, preventing the mixing with ambient air. In Figure 18B is shown a store chamber's design detail, while in Figure 18C is shown the store chamber with the gas sensors placed within it. The store chamber's dimension was fixed at about 600ml, according to pulmonary capacity. The store chamber is provided also with a flushing pump (see Figure 18D) which allows to purge the chamber itself, after each measuring. A sampling circuit injects, at a certain rate (=120 ml/sec, basing on [3]), the exhaled gas samples in a second chamber, where the two COSMED gas sensors (one sensitive to oxygen, the other sensitive to carbon dioxide, both working in flow) are placed.

To link the gas sensors with other electronics, in order to send the collected data to Arduino board, and then to the computer, we thought about a kind of twin lead.

An important aspect for the functionality of the WS is that the chamber embedding the sensors could be opened easily, in order to be able to change the sensors, if necessary. All the different steps during the design of the WS were considered at the light of this basic requirement.

The final configuration of the Wize Sniffer 1.0 is shown in Figure 18D, the reverse side of the box is shown in Figure 19, while in Fig.20 is shown an example of its employment.

Box dimensions are: 30cm x 38cm x 14cm.

The device requires a voltage supply of 12V.

A

B

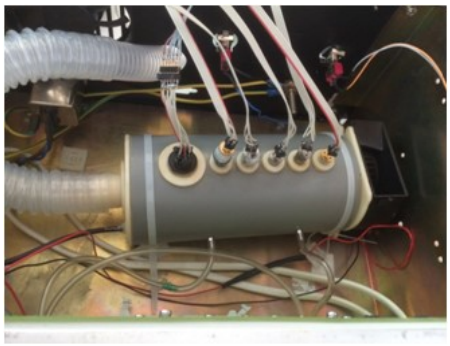

C

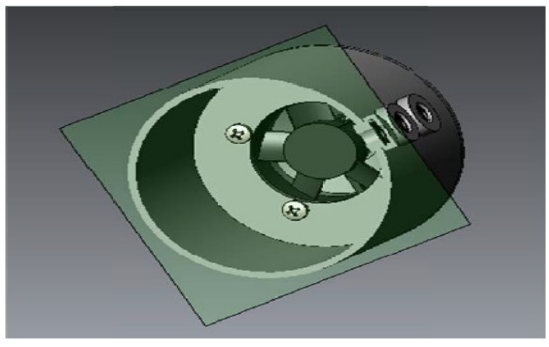

D

Fig. 18. From A to D, examples of the components of the WS. A: corrugated tube; B: store chamber, 600ml; C: store chamber with gas sensor located inside; D: flushing pump.

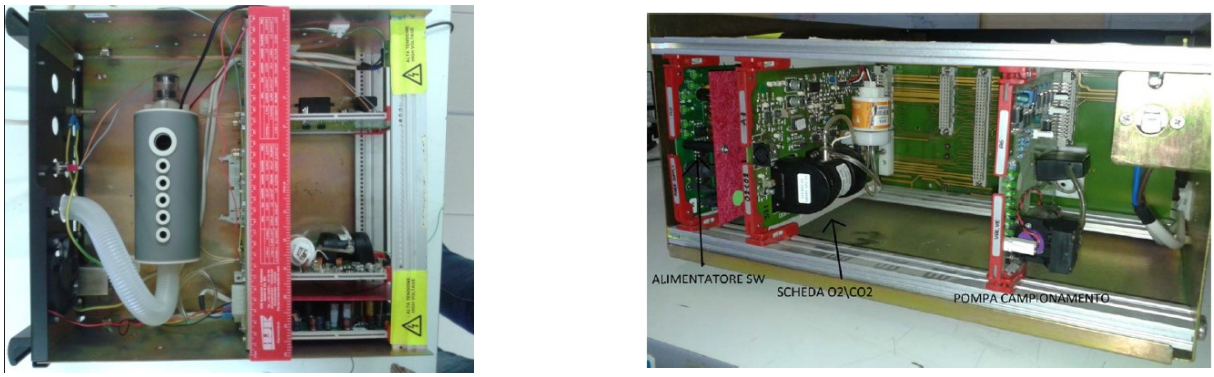

Fig. 19. WS: panoramic view from the top of the interior.

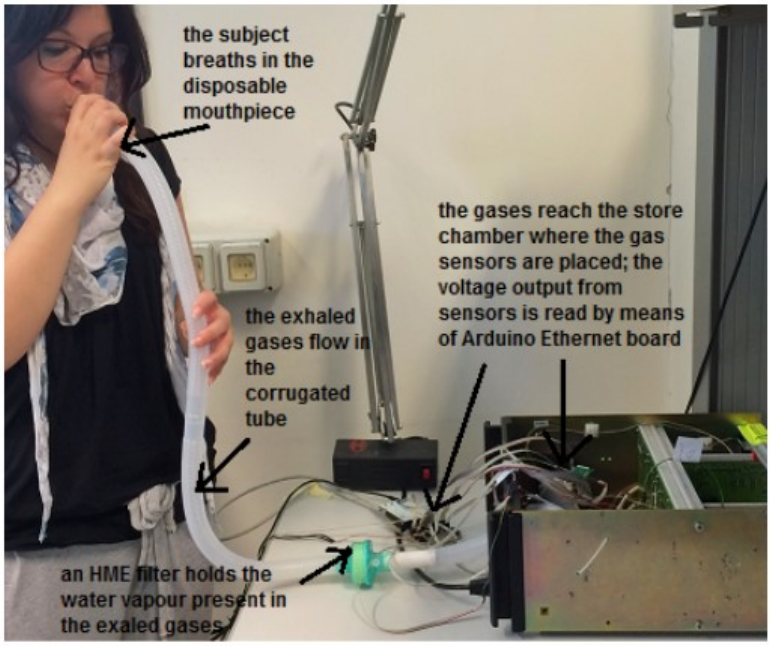

Fig. 20. The working WS as used by an end-user.

4.5 The circuit and Arduino board

In order to receive the data from the sensors, we decided to make use of a microcontroller board, an Arduino board. Initially, the choice of the type of Arduino board has been made taking into account:

- Number of bits of analogue-to-digital converter;
- Number of analogue input pins;
- Possibility to use an Ethernet module.

This last requirement was due to the advantage of sending the data from Arduino to computer wireless. Our aim was to create a Telnet server by using Arduino, in order to read data by making a simple request to the server itself from our computer. These aspects will be described in detail in the section referring to the software- data communication protocol.

Based on these requirements, the choice fell initially on Arduino Ethernet board (Figure 21).

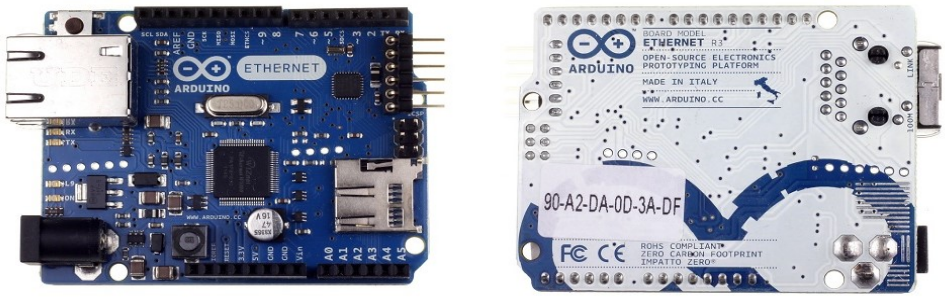

Fig.21. An Arduino Ethernet.

Arduino Ethernet has 14 digital input/output pins (but 4 of them are reserved for interfacing with Ethernet module, soothe number of available pins becomes 9); 4 of the digital pins are available as PWM outputs. It has 6 analogue input pins, each of which provides 10 bit of resolution (=1024 different values). Recommended input voltage is 7-12V.

After choosing the microcontroller board, we have realized the electronic circuit. The sensors to read was: 6 Figaro gas sensors + 2 COSMED gas sensors + Sensirion temperature and humidity sensor. As a consequence, first of all, it was necessary to integrate a multiplexer (CD4051B, Texas Instrument), in order to switch the reading output as need be. A scheme of CD4051B is shown in Figure 22.

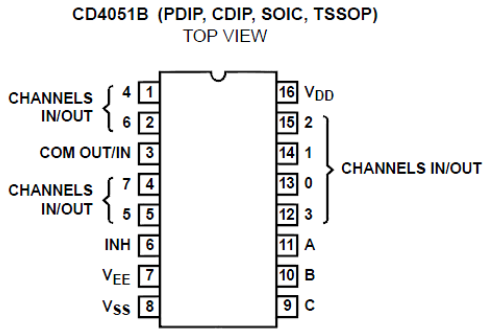

Fig.22. Scheme of Arduino CD4051B pins.

To avoid the influences that the measuring circuit have on the source itself, and hence on the sensors' output, we have integrated 8 buffers, one for each analogue output. Indeed, output values from the sensors have been sent to buffers' input, while the buffers' output have been sent to Arduino analogue input pins. In this way, the voltages output from the gas sensors was stabilized, too.

The type of buffers we have chosen was LM124-N manufactured by Texas Instrument. An example of its scheme is shown in Figure 23.

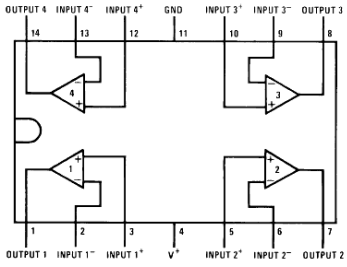

Fig.23. Example of the buffer LM124-N manufactured by Texas Instrument

Subsequently, we have integrated the slots for the sensors. Each slot has 4 holes:

- One for the voltage supply, to power the sensor, if it needs (in the case of Figaro sensors and of the Sensirion, it must be equal to 5V);
- One for the heater voltage, to heat the sensor (this is necessary only for Figaro sensor and it is equal to 5V); in the case of Sensirion, this connection has been used to connect the sensor's pin reserved to the clock, to Arduino clock pin.
- One for the data output;
- One for the GND.

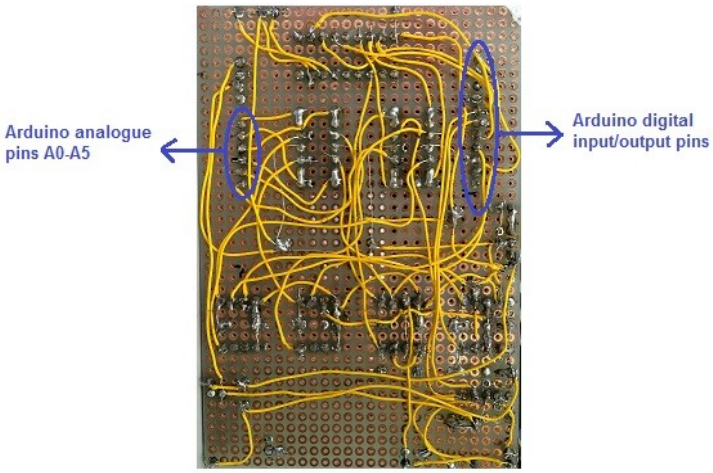

Fig. 24. The front of the electronic board.

The power circuit and the heater circuit were separated, because the second required more current than the first and overloaded the power supply. So, for the power circuit a power supply of 9V and a voltage stabilizer with an output of 5V have been used, while for the heater circuit a power supply of 5V has been used. Figure 24 shows the circuit (front) and Figure 25 shows the circuit (back).

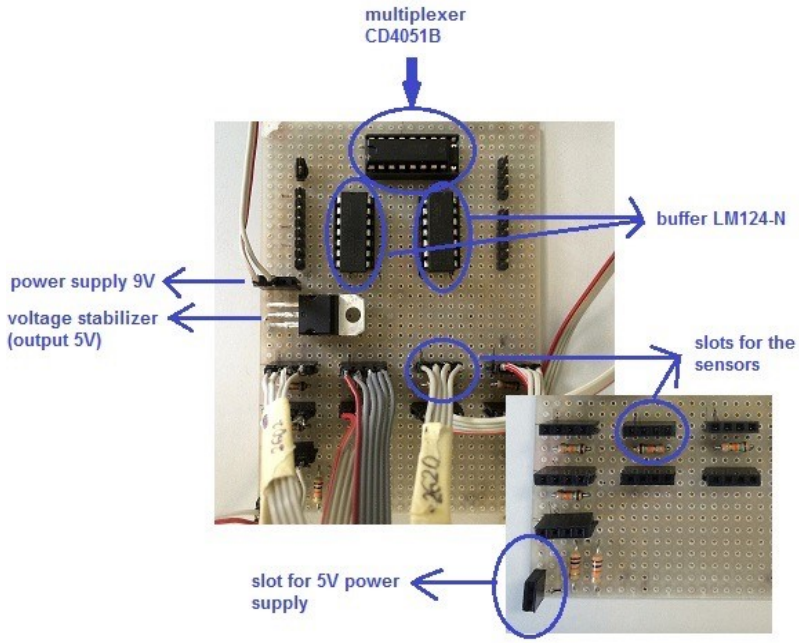

Fig.25. The back of electronic board.

A 15KΩ load resistances (RL) has been used for Figaro gas sensors.

The general scheme of the circuit realized is shown in Figure 26 and the final configuration of the Wize Sniffer 1.0 with its electronics is shown in Figure 27.

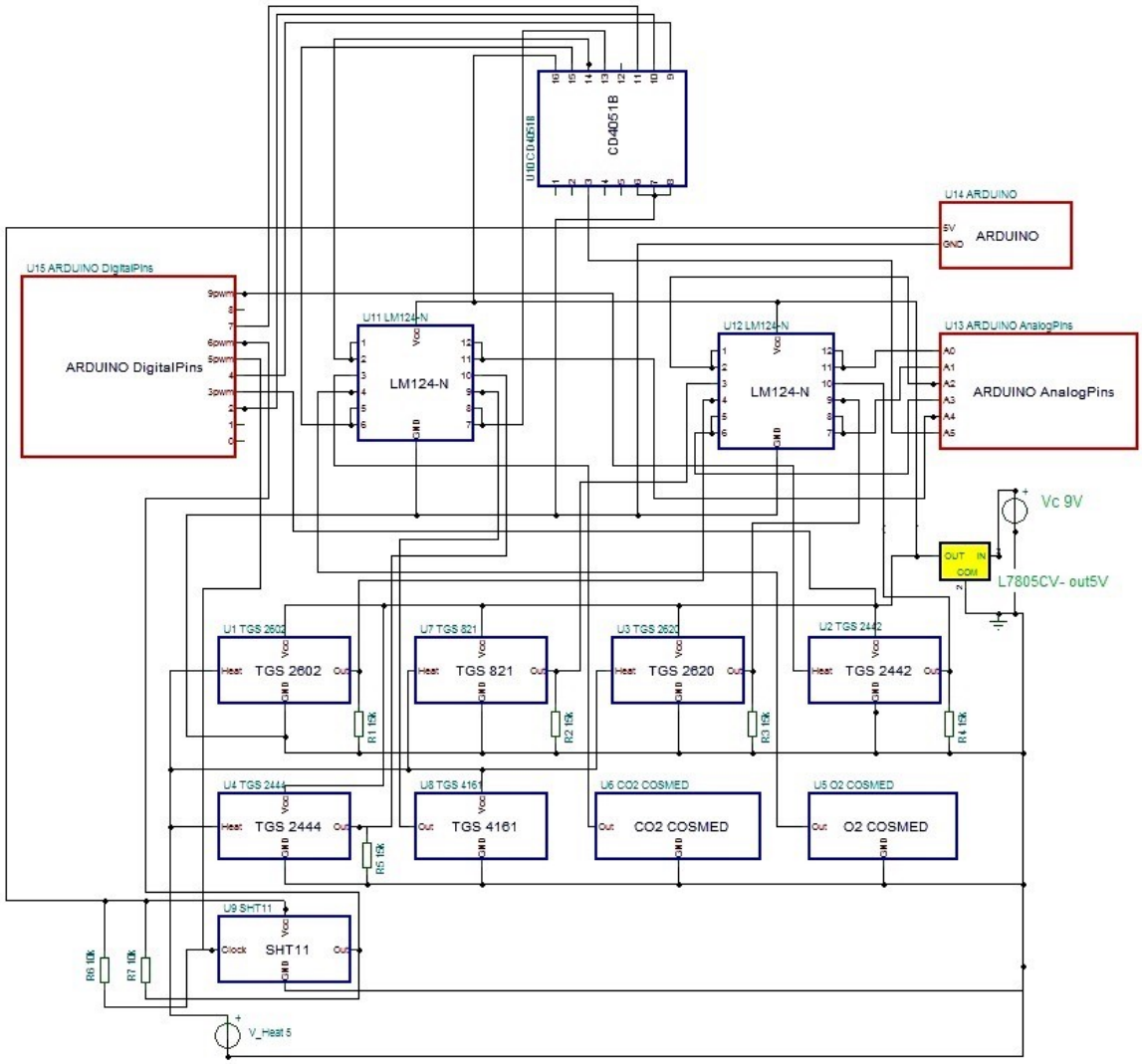

Fig.26 The general scheme of the circuit realized

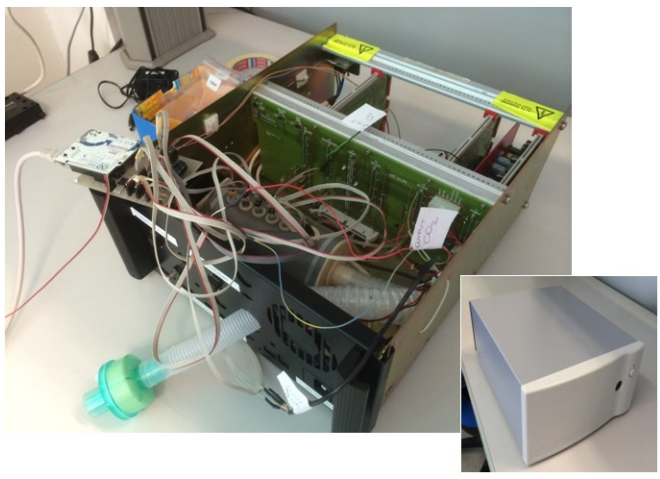

Fig. 27. The Wize Sniffer 1.0 with all the components and as it appear to the end user (in inset).

4.6 THE COMMUNICATION PROTOCOL BETWEEN ARDUINO AND PC

Usually, when Arduino board is used to read data from sensors, or from other devices, a USB cable is the most simple way to communicate a personal computer with Arduino itself. Nevertheless, this is not very advantageous if the computer is placed far away from Arduino. A wireless connection between the devices become necessary; that is because initially we have chosen a model of Arduino with Ethernet module. The idea we had can be explained as in Figure 28.

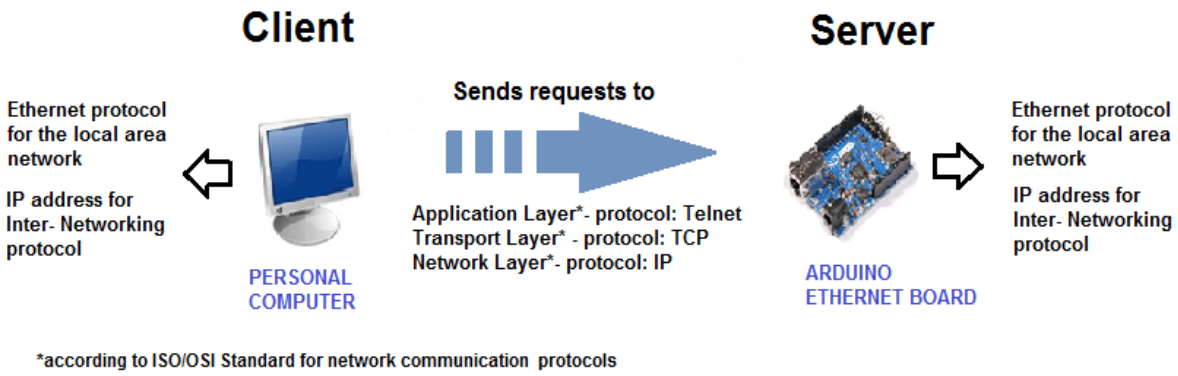

Fig. 28. Schematic protocol of the communication protocol.

First, we programmed Arduino Ethernet board in order to create a Telnet Server. Telnet is a client-server protocol, based on TCP protocol, pertaining to application layer, according to ISO/OSI Standard for Network Communication Protocols. Usually, a client makes a connection to server's port 23.
The pseudocode of the program on the Arduino Ethernet board with the aim to create a Telnet Server is as follows:

✓ Uploading Ethernet libraries, network configuration, setup() function
- *<Ethernet.h>,* Arduino mac Address, Arduino IP Address
- *EthernetServer server = EthernetServer(23); // telnet defaults to port 23*
- *Ethernet.begin (mac, ip); // initialize the ethernet device*
- *server.begin(); // start listening for clients*

✓ *Loop() { if (client==true)*, there will be bytes available to read:
- *out(i) = analogRead(i)*0.0049; // reading Analogue Pin values*
- *client.print(out(i)); // print of the 8 sensors' values (Volts)*

Subsequently, to send a request to this Telnet Server, and receive data from it, we created a TCP/IP object implemented in Matlab. It allows to make a connection to server's port 23 and fill the buffer (which dimensions can be set) with the data coming from the server. It means, the buffer is filled with the sensors' values array.
Moreover, the data received can be saved in a text file in order to be managed for further analysis.
The pseudocode of the program written in Matlab ® is as follows:

✓ Opening connection and reading a "tcp/ip object"
- *t = tcpip('Arduino IP Address' , 23); // connect to (port 23) Arduino*
- setting (t, Buffer dimension, other properties);
- *fopen(t) ; // start connection*

- ❖ Until there will be 'BytesAvailable' - -> *A= fscanf(t)*

✓ Saving the data
- ❖ *fprintf (fileID, A); // writing the data read in a file .txt*

✓ Closing connection
- ❖ *fclose(t);*

Details on the code operating on Arduino to read the values from the sensors are shown below.

4.6.1 READING THE VALUES FROM THE SENSORS

The loop code on Arduino Ethernet board necessary to read the values coming from the different sensors (Figaro gas sensors, COSMED gas sensors and Sensirion temperature and humidity sensor) is shown below as a pseudocode:

✓ Out of the loop, 10 variables "float" are declared
- ❖ *float "out(i)";*

✓ Setting the multiplexer control inputs (Arduino's pin7, pin2, pin4) according to the input to read es:
- ❖ *digitalWrite(7, LOW); //setting mux control input*
- ❖ *digitalWrite(2, LOW);*
- ❖ *digitalWrite(4, LOW);*

✓ The gas sensors' output is sent in input to Arduino analogue pins; so, to read them:
- ❖ *out(i) = analogRead(i)*0.0049;*

✓ For the TGS2442 it was necessary to set the digital pins to heat and sense the sensor itself by a pulse heating/powering cycle (as described in the section referring to the hardware-gas sensors). For the TGS2444, on the contrary, this was not necessary, so, it was powered with a continuous power source, as for the others Figaro sensors.
- ❖ *digitalWrite(3, LOW);*
- ❖ *analogWrite(9, 245);*
- ❖ *delay(14);*
- ❖ *analogWrite(9, 0);*
- ❖ *delay(981);*
- ❖ *digitalWrite(3, HIGH);*
- ❖ *delay(3);*
- ❖ *out0 = analogRead(0)*0.0049; //0.0049 is the bits' resolution in Volt*
- ❖ *digitalWrite(3, HIGH);*
- ❖ *digitalWrite(3, LOW);*

✓ For the Sensirion SHT11 it was necessary to load its libraries to read it:
- ❖ *#include <SHT1x.h> //for SHT11 (humidity and temperature sensor)*
  #define dataPin 6
  #define clockPin 5
  SHT1x sht1x(dataPin, clockPin);
  temp_c = sht1x.readTemperatureC();
  humidity = sht1x.readHumidity();

From .txt file to plot using a Matlab code

The data received from server and saved in a text file can be managed for further analysis. So, it may be advantageous re-shaping them in a matrix:

✓ Opening data text file and creating a matrix of values:
- ❖ *fopen ('data.txt');*

- ❖ re-shaping of the data the file in a matrix :

mat[x rows, 10 columns (=number of sensors)]

- ✓ From matrix àto vectors (one for each sensor) à …
- ❖ *SENSOR(i)=(mat(:,(i))';*
- ✓ … to plot

In Figure 29 is shown an example of a plot (volts *vs* time) of the 6 Figaro gas sensors reporting the data from an individual breath measurement.

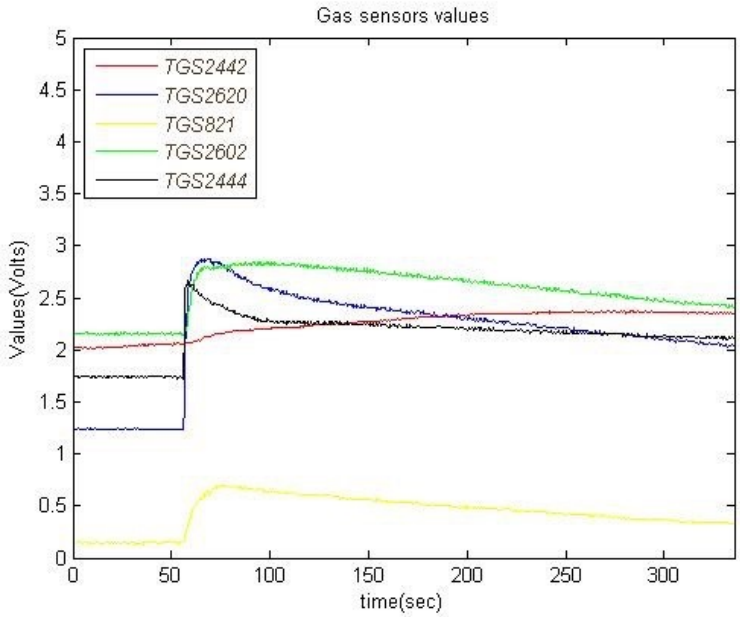

Figure 29. Example of a plot (Volts vs time) of the 6 gas sensors reporting the data from an individual breath measurement.

5. WIZE SNIFFER 1.0 PERFORMANCE TEST

After having developed this first prototype of Wize Sniffer, the next step was to test it in order to evaluate its performances and make it ready to be integrated in the ”Wize Mirror”.
For this purpose, first we tested each gas sensor singularly, making them sense the several substances (on the order of picoliter) they are sensitive to; then, The Wize Sniffer 1.0 was tested using a population containing individuals of different age, habits, body type.

5.1 SINGLE TESTS

The only aim of these tests was to evaluate sensors' response on a quality level. That is, only evaluate their change, their rise in voltage outputs when sensing that/those gas/gases they are sensitive to. Here an example of outcome is described, relative to the test conducted on TGS2602.
Each sensor was placed, together with the temperature and humidity sensor (Sensirion SHT11) in an airtight desiccator, as shown in Figure 30. The substances, which the sensors are sensitive to, were placed, one by one, in the desiccator; they were on the order of picoliter. The data from sensors were registered and saved by means of a personal computer.

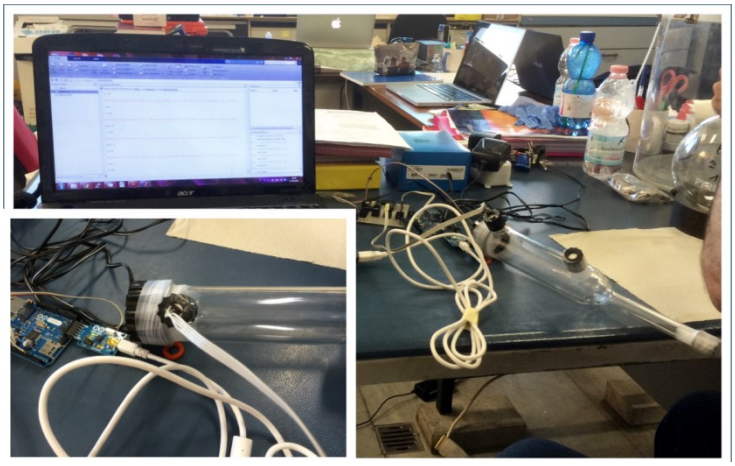

Fig.30- Experimental set-up for selectivity gas sensors (with the useful support of Tommaso Lomonaco and Silvia Ghimenti, form the University of Pisa and IFC-CNR)

For **TGS2602** (sensitive to hydrogen, ammonia, ethanol, hydrogen sulfide, toluene) pico-liters of ethanol, ammonia, toluene were placed on the bottom of desiccator, one by one. It was not possible to involve hydrogen and hydrogen sulfide in the tests. The voltage outputs are shown in Figure 31. It should be noted how the voltage values in response to ethanol and toluene rose faster than in response to ammonia. Similarly, the peak values relative to ethanol and toluene were higher than the one corresponding to ammonia. This is in line with the slopes of bilogarithmic curves mapping the sensor sensitivity characteristics for the several substances. Indeed, TGS2602 sensitivity characteristic for ethanol shows a slope $\alpha_{TGS2602Eth}$ equals to -0.416939 (just as for toluene, $\alpha_{TGS2602Tol}$ equals to -0.564573), whereas for ammonia $\alpha_{TGS2602NH3}$ is -0.28658).

Temperature and humidity values were constant at about, respectively, 23°C and 70%.

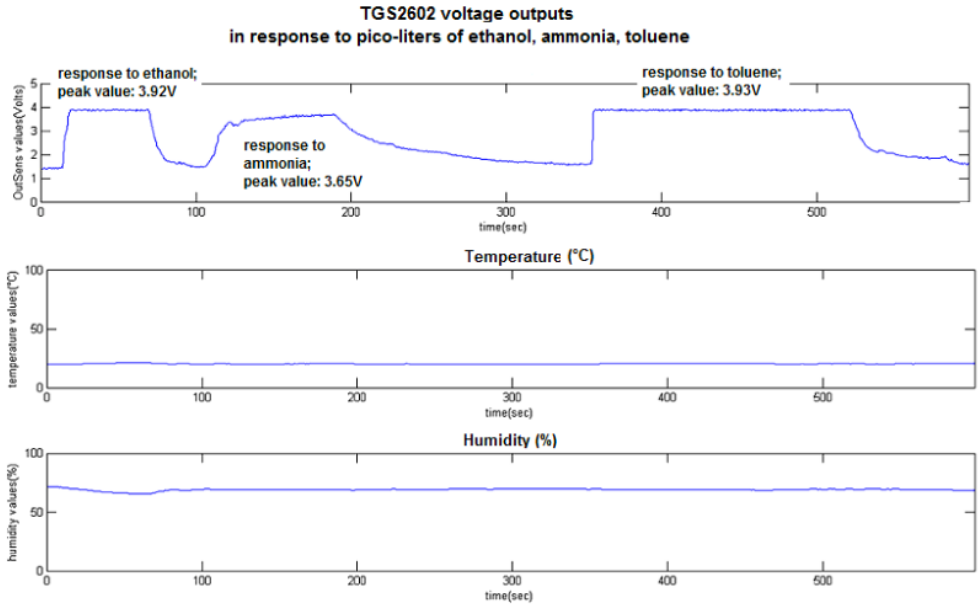

Fig.31- TGS2602 outputs in response to ethanol, ammonia, toluene concentrations on the order of pico-liters. It should be noted how the voltage values in response to ethanol and toluene rose faster than in response to ammonia. Similarly, the peak values relative to ethanol and toluene were higher than the one corresponding to ammonia. This is in line with the slopes of bilogarithmic curves mapping the sensor sensitivity characteristics for the several substances. Temperature and humidity values were constant at about, respectively, 23°C and 70%.

5.2 TEST ON INDIVIDUALS

A second phase of our trials has been focused on the evaluation of device's performances when used to sense human exhaled gases.
For this purpose, two important aspects were taken into account:

- the target population: the atherosclerotic illness develops insidiously, and clinical manifestations often become evident in its advanced stages. Altogether, the correlated diseases and complications occur between 40 and 60 years of age. As a consequence, since it's talking about prevention, we considered a population between 20 and 40 years of age, containing individuals with different habits (smokers/non smokers, sporty/sedentary lifestyle, healthy/unhealthy diet, teetotal/social drinker).
- the methodological issues about sampling procedure. In practice are often used three methods of sampling: "alveolar (end-tidal) sampling" (which corresponds to the plateau of the CO2 curve, that is the maximum value of exhaled CO2),"mixed expiratory air sampling" (which corresponds to a whole breath sample),"time-controlled sampling" (which corresponds to a part of exhaled air sampled after the start of expiration). Controlled alveolar sampling by means of expired CO2 concentrations is the method of choice if systemic volatile biomarkers are to be assessed, since only alveolar compounds are correlated to compounds in blood. The mixed expiratory air sampling, without controlled identification of the respiratory phases bears the risk of dilution with dead space air, but this

method allows to collect also the compounds of exogenous origin. The last method shows large variations of compositions because of wide variations of individual dead space volumes and breathing maneuvers, then it is less used in clinical practice. For our purposes, mixed expiratory air sampling method was chosen, since our interest was focused on endogenous biomarkers, but also to the compounds of exogenous origin (ethanol, for example). Additionally, since the composition of single breaths may vary considerably from each other, because of different modes and depth of breathing, in order to have, in this work phase, breath samples that were as reproducible as possible, we preferred a sampling of multiple breaths (three breaths).

The individuals were divided in two age-groups: [20-30 years old] and [30-40 years old]).
The tests were run following subjects' habits and lifestyle.

Basing on these considerations, the test allowed us to:

- **Evaluate whether the device is able to discriminate between two different alcoholic grades**
- The data relative to the blood alcohol concentration were registered also by means of a simple alcohol tester.
- **Evaluate whether the device is able to discriminate different amounts of the same drink**
- The data relative to the blood alcohol concentration were registered also by means of a simple alcohol tester.
- **Assess whether the device is able to follow the trend in time of the alcohol disposal**
- The data relative to the blood alcohol concentration were registered also by means of a simple alcohol tester.

Assess whether the device is able to discriminate between non smoker's exhaled gas and smoker's exhaled gas

- **Evaluate device's output in response to a subject's exhaled breath after smoking**
- **Evaluate device's output in response to a subject's exhaled breath after smoking and drinking alcoholic drink**
- **Evaluate device's output in response to:**
- overweight subject's exhaled breath;
- normal body type subject's exhaled breath;
- subject's exhaled breath after exercise.

The test data, that is, the voltages output from the gas sensors, were sent to pc by means of a TCP/IP communication protocol and saved in text files (.txt). Then, the data were analyzed by means of a program implemented on Matlab. This program allows to calculate substances concentrations from the voltage values, basing on the sensors sensitivity curves. The pseudocode is the following:

✓ Opening data text file and creating a matrix of value:
- ❖ *fopen ('data.txt');*
- ❖ re-shaping of the data in a matrix:

mat[x rows, 10 columns(=number of data to be read)]

✓ From matrix —> to vectors (one for each sensor)
- ❖ *SENSOR(i)=mat(:,(i));*

avg(i)=(sum(SENSOR(i)(1:9))/(length(SENSOR(i)(1:9)));

SENSOR(i)=SENSOR(i)-avg(i); %set baseline values to zero

- ✓ For each "gas sensor vector", the maximum voltage value is saved in another vector V:
  - ❖ *V(i) = max(SENSOR(i));*
- ✓ From voltage value —> to Rs—> to Rs/Ro ratio…
  - ❖ *Rs(i)=((Vc-V(i))/V(i))*Rl; %Voltage divider equation*
  - ❖ *RATIO(i)=Rs(i)/Ro(i);*
- ✓ to substances concentrations by means of "mysyst" function, created ad-hoc
  - ❖ *CONC(i)=(RATIO(i)/A_{j_sub})^(1/$alpha_{j\_sub}$);*
- ✓ Data plot

This program opens the file .txt where the sensors' voltage outputs has been saved, and reshapes them in a matrix containing 10 rows (everyone corresponding to each sensor: TGS2442, TGS2660, TGS821, TGS2602, TGS2444, TGS4161, Cosmed CO2 sensor, Cosmed O2 sensor, temperature values, humidity values). Then, creates vectors 1xn, each of which corresponding to a specific sensor. The baseline values are set to zero, and for each vector the maximum voltage value is saved in another vector.

Since the ones manufactured by Figaro are semiconductor gas sensors, which functioning is based on a variation of internal resistance (Rs) when they sense gas molecules, then this Rs had to be calculated (except for TGS4161) starting from the output voltage, according to the voltage divider equation present in the datasheets (1):

(1)
$$Rs = RL\frac{Vc - V_{out}}{V_{out}}$$

where *RL* is the load resistance on which the V_{out} is taken, and *Vc* is the sensor power supply. In addition, the ratio R_s/R_0 (where R_0 is the resistance reference value and it is different for each sensor) had to be calculated, according to sensors' sensitivity characteristics which map the ratio R_s/R_0 as a function of the substance concentration. In particular, these sensitivity characteristics derive from a power low such as (2):

(2)
$$\frac{Rs}{Ro_{TGSxxxx}} = A_{TGSxxxx_{sub}}[sub]^{\alpha_{TGSxxxx_{sub}}}$$

The constant parameters $A_{TGSxxxxsub}$ and $\alpha_{TGSxxxxsub}$ are different for each sensor. They has been calculated fitting the bilogarithimc curves representing the sensitivity characteristics. For this purpose, the software "Gnuplot" has been used. Starting from the knowledge, for each Figaro sensor, of the ratio Rs/Ro, and of the constant parameters $A_{TGSxxxxsub}$ and $\alpha_{TGSxxxxsub}$, the function "mysyst" calculates the concentrations of the substances detected by TGS2442, TGS821, TGS2620, TGS2602, TGS2444, according to the following system of non-linear equations (3)

$$\begin{cases} (\frac{Rs}{Ro})_{2442} = A_{2442_{\mathrm{CO}}}[\mathrm{CO}]^{\alpha_{2442_{\mathrm{CO}}}} \\ (\frac{Rs}{Ro})_{821} = A_{821_{\mathrm{H_2}}}[\mathrm{H_2}]^{\alpha_{821_{\mathrm{H_2}}}} \\ (\frac{Rs}{Ro})_{2444} = A_{2444_{\mathrm{NH_3}}}[\mathrm{NH_3}]^{\alpha_{2444_{\mathrm{NH_3}}}} \\ (\frac{Rs}{Ro})_{2620} = A_{2620_{Eth}}[Eth]^{\alpha_{2620_{Eth}}} + A_{2620_{\mathrm{H_2}}}[\mathrm{H_2}]^{\alpha_{2620_{\mathrm{H_2}}}} + A_{2620_{\mathrm{CO}}}[\mathrm{CO}]^{\alpha_{2620_{\mathrm{CO}}}} \\ (\frac{Rs}{Ro})_{2602} = A_{2602_{Eth}}[Eth]^{\alpha_{2602_{Eth}}} + A_{2602_{\mathrm{H_2}}}[\mathrm{H_2}]^{\alpha_{2602_{\mathrm{H_2}}}} + A_{2602_{\mathrm{H_2S}}}[\mathrm{H_2S}]^{\alpha_{2602_{\mathrm{H_2S}}}} + A_{2602_{\mathrm{NH_3}}}[\mathrm{NH_3}]^{\alpha_{2602_{\mathrm{NH_3}}}} \end{cases}$$

(3)

This system resulted from three hypothesis:

- for the ”multi-sensing” sensors (TGS2620 and TGS2602), we made the hypothesis that the several contributions from the several substances add together linearly;
- TGS2620 is sensitive to methane and isobutane, too. Since the sensitivity range for methane and isobutane (50-5000ppm)is higher than the amounts of these substances present in our breath (less than 2 ppm), we made the hypothesis that their contributions were null; so:

$A_{2620CH4[CH4]}{}^{\alpha}{}_{2620CH4} = 0$

$A_{2620Isob[Isob]}{}^{\alpha}{}_{2620Isob}=0$

- The same, for the toluene, which TGS2602 is sensitive to. TGS2602’s sensitivity range for toluene is 1-10ppm, while in our breath this com- pound is present in lower amounts (less than 1 ppm); so (for our purposes) we can considered null also the quantity:

$A_{2602Tol\ [Tol]}{}^{\alpha}{}_{2602Tol} = 0$

The assessment of the CO_2 concentration, detected by TGS4161, results from the equation:

$$[CO_2] = 1000V_{out} \qquad (4)$$

For the sensors of CO_2 (IR1507 Servomex (www.servomex.com)) and O_2 (MOX20 (CityTechnology -- www.citytech.com)) supplied by COSMED, CO2 and O2 concentrations can be assessed by means of the following table

CO_2	O_2
0.02V +/-0.01V @ 0.03%	0 to 4V+/-0.01V @20.93%
1.75V +/-0.01V @ 2.00%	
3.5V +/-0.01V @ 5.00%	

Figure 32. Sensitivity of the CO2 (IR1507 Servomex) sensor and O2 (MOX20 City technology).

Finally, the program implemented on Matlab allows to plot the data, mapping, for each sensor, the voltage output as a function of time (naturally, according to the test period).
As well known, there will be an increase in voltage if the sensor senses the gas which is sensitive to; the maximum voltage value will be related to the amount of substance that the sensor sensed.

The most meaningful results are reported, and the "Wize Sniffer 1.0" performances are discussed as well.

1. **Healthy subject: typical curves**

The test is relative to a non-smoker, teetotal, female subject belonging to the age range [30 - 40], having normal body type.

The results relative to breath gases concentrations are shown in table 2. In the table, the baseline concentrations are shown for each substance. It should be noted that these baseline values are purely approximate and indicative: the one of "breath analysis" is a very innovative field, so, the gases' concentration range, that might be attributed to a healthy subject's exhaled breath, are not still standardized.

	HR(Bpm)	[CO]ppm	[H2]ppm	[Eth]ppm	[H2S]ppm	[NH3]ppm	[CO2]ppm	[CO2]C	[O2]ppm
BL	60-70	0.6-4.9	0.3-34.1	0-3.9	0-1.3	0-1.3	4000	4%	14%
S1	70	4.49	9.99	1.95	0.62	0.42	3380	4.4%	16.39%

Table 2 – Exhaled molecules' concentrations by a healthy (or asymptomatic) subject; in the first row, the indicative baseline levels for each substance.

2. **Evaluation whether the device is able to discriminate different amounts of the same drink and to follow the trend in time of alcohol disposal**

The test is relative to a non-smoker, social drinker, male subject belonging to the age range [20-30], having normal body type. The results relative to breath gases concentrations are shown in table 3. As we expected, the voltage outputs showed an increase after the first and then after the second alcoholic drink, and a decrease when alcohol disposal began.

	Wize Sniffer [Eth]ppm	Alcolino126 BAC	Alcolino126 BrAC
Without alcohol intake	3.86	0.00mg/l	
20min. after 1st 100ml of wine	30.98	120mg/l +/- 10%	33.66ppm +/- 10%
20min. after 2nd 100ml of wine	69.31	280mg/l +/- 10%	73.88ppm +/- 10%
after 20min	39.81	160mg/l +/- 10%	42.27ppm +/- 10%
after 40min	20.28	110mg/l +/- 10%	29.95ppm +/- 10%
after 60min	11.36	50mg/l +/- 10%	13.22ppm +/- 10%

Table 3- Alcohol intake: different amount of the same drink (same alcoholic grade)and alcohol disposal-Wize Sniffer 1.0 output ethanol concentration and Alcolino output Blood Alcohol Concentration (BAC). From BAC value, the BrAC one can be estimated.

An interesting result was given by hydrogen sensor: coherently with bibliography [1], there was a decrease in concentration values when the subject drank alcohol, and a return to initial values in the following 20-40 minutes. This is shown in Figure 33 and 34, which reported also an example of *breath curves.*

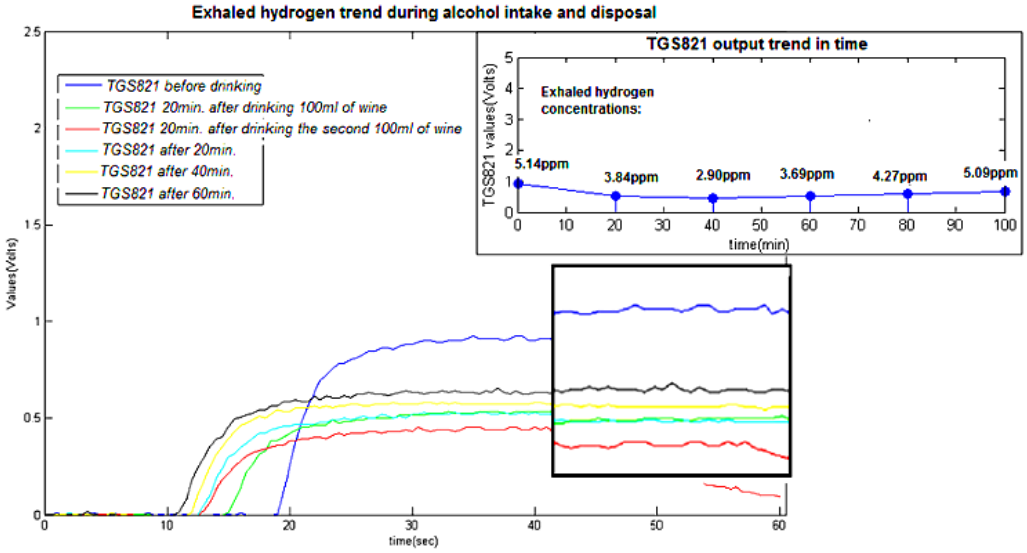

Fig.33- The change in exhaled hydrogen concentrations can be seen clearly in the plot mapping the trend in time.

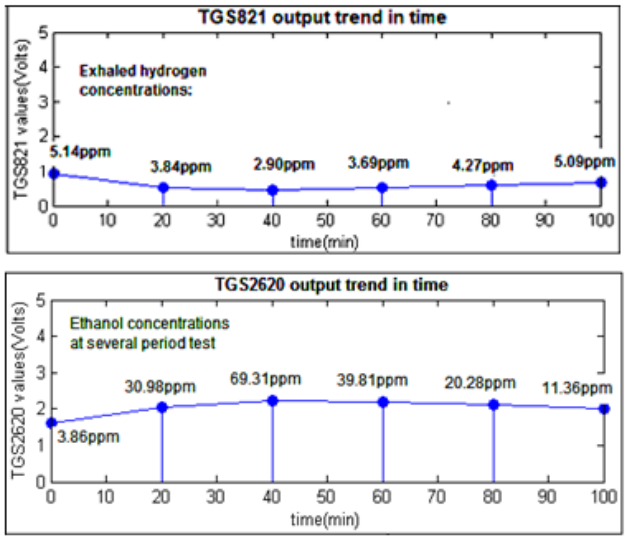

Fig.34– Trend in time of hydrogen and ethanol concentrations during alcohol intake and alcohol disposal

3. Evaluation whether the device is able to discriminate between moderate smoker subject and non-smoker subject's exhaled gas; Evaluation also the device's output in response to a subject's exhaled breath after smoking and after smoking and drinking.

The tests are relative to a non-smoker female subject belonging to the age range [30-40], having normal body type, and to a moderate smoker female subject, belonging to the same age range, having overweight body type.

First, the non smoker subject made 3 wholes breath into the device by means of the corrugated tube. The test was repeated on the smoker subject. Then, another two tests were conducted: respectively, after the smoker subject smoked a cigarette, and after the same subject smoked and drank 100ml of beer.

The results relative to breath gases concentrations are shown in Table 4.

	HR(Bpm)	[CO]ppm	[O2]ppm	[CO2]ppm	[CO2]C	[H2]ppm	[Eth]ppm	[NH3]ppm
non-sm. subj	78	4.49	18.33%	3320	3.77%	3.49	1.24	0.41
sm. subj	79	9.19	17.4%	3370	3.95%	1.39	1.86	0.26
sm. subj after smoking	77	20.7	16.84%	3398	4.14%	3.462	2.007	0.46
sm. subj after smoking and drinking	77	30.04	15.90%	3368	4.4%	2.47	12.7	0.89

Table 4- Smoking habit: discrimination between non smoker subject and moderate smoker subject; effects of smoking on exhaled gas

Several considerations derived from these trials can be summarized as follows:

- the device was able to discriminate between a non-smoker subject and a moderate smoker subject; indeed, the values corresponding to carbon monoxide concentrations, just like the ones corresponding to carbon dioxide, were higher in a smoker individual than in a non-smoker; as a consequence, the oxygen concentrations followed the opposite trend, coherently to the fact that carbon monoxide in blood takes the place of oxygen, forming a more stable bond with haemoglobin;
- after smoking, both the times, the device detected higher values not only of carbon monoxide but also of ammonia, coherently to the presence of ammonia in cigarette smoke;
- the ethanol concentrations (12.7ppm) after alcohol intake (100ml of beer- alcoholic grade= 5%) were very close to the ones detected by means of alcohol tester (which returned an output of 0.06g/L for BAC, corresponding to 15.87ppm for BrAC);
- a limit for the detection of carbon monoxide could be the very low TGS2442 response time; although having good performance, the sensor was too slow not only in the response, but also while coming back to its baseline value;
- The working performance of the COSMED sensor for carbon dioxide was better than the one given by TGS4161 (Figaro sensor for carbon dioxide), that saturated too quickly. This may be due to Cosmed CO2 sensor detection range which is wider than the one of TGS4161. As a consequence, the first was able to discriminate between smoker's exhaled CO2 and non-smoker's exhaled CO2, more than the second one;
- An interesting aspect regarding the detection of exhaled hydrogen, was that exhaled hydrogen showed an increase after smoking, and a decrease after alcohol intake, coherently with bibliography [21].

4. Metabolism: evaluate device's output in response to:

- overweight subject's exhaled breath;

- normal body type subject's exhaled breath;

- subject's exhaled breath after exercise;

The tests are relative to a normal body type male individual belonging to the age range [20- 30], and to an overweight female subject belonging to the same age range.
First, the subjects have made 3 wholes breath into the device by means of the corrugated tube. Then, the test has been repeated on the overweight subject, after exercise. The results relative to breath gases concentrations are shown in Table 5.
Higher values of exhaled hydrogen (correlated, as known, with carbohydrates fermentation) can be found, as in table 4, in individuals suffering overweight problems. On the contrast, after running, there is a decrease in value for exhaled hydrogen.
In addition, in the study conducted by D.G. Thompson et al.,[21], it was found that exhaled hydrogen showed a decrease in value after exercise. The higher ventilation rate, because of exercise, reduces hydrogen concentration in the lungs.

	HR(Bpm)	[Eth]ppm	[H2]ppm
Subj 1	57	1.41	5.49
Subj 2	93	3.04	16.77
Subj 2 after running	140	2.07	6.173

Table 5- Metabolism: device output concentration relative to exhaled ethanol and hydrogen- comparison between normal body type subject (SUBJ1) and overweight subject (SUBJ2)

As a consequence, also in our trial here was a decrease in exhaled hydrogen "washed out" from the lungs by higher ventilation rate caused by running. Naturally, there was a rise also in exhaled carbon dioxide values: 4.28% before running versus 5.39% after running.

5.2.1 Preliminary validation of results

From the tests, we gathered that the device is able to provide reliable outputs on a quality level. In order to evaluate whether also its quantitative outputs were in line with bibliography, we considered worthwhile to validate our results comparing them with the ones output by Gas Chromatography and the ones (relative to carbon monoxide) output from piCO+ Smokerlyzer.

Validations of results by means of gas chromatography
We were able to validate only the results correspondent to the exhaled ethanol detection. Indeed, the gas chromatograph used was able to detect molecules with a molecular weight higher than 40g/mol. Then, our attention has been focused on the comparison between exhaled ethanol concentrations output from Wize Sniffer, and the ones analyzed by means of gas chromatograph. The test was performed as follows:
Three subjects were taken from the population described previously: a female subject (SUBJ1) quasi-teetotal, a male subject (SUBJ2), social drinker, and a female subject (SUBJ3), social drinker. All of them were normal body type and belonging to the age range [30- 40].
Naturally, the Wize Sniffer returned a real-time output, whereas the gas chromatography requires about 1hour for each sample.

Gas Chromatography results

The results relative to exhaled ethanol concentrations obtained using the gas chromatograph are shown in Table 6.

	Ethanol Area	Ethanol concentration (ppmv)
SUBJ 1- PRE SUBJ 1 - POST beer	< LOD 4.44E+07	< LOD 46.8
SUBJ 2- PRE SUBJ 2 - POST prosecco	< LOD 3.46E+0.7	< LOD 36.5
SUBJ 3- PRE SUBJ 3 - POST wine	< LOD 4.28E+07	< LOD 45.1

Table 6- Gas Cromatography results. In the first column, the areas under peaks are shown; in the second one, the exhaled ethanol concentration (in ppmv) are reported.

The ethanol concentrations relative to the first test (that is, before alcohol intake), were under LOD (limit of detection). The difference between alcoholic grade was underlined by SUBJ2 and SUBJ3 exhaled ethanol. Nevertheless, this comparison should not be made because alcohol disposal varies between individuals and depends on several factor, among which sex, age, body mass, body fat, alcohol intake habit. Indeed, this was underlined by SUBJ1, quasi-teetotal, that is, little used to alcohol intake, who drank beer (which generally has an alcoholic grade lower than the wine) and exhaled more ethanol than SUB1 and SUBJ2.

Wize Sniffer results

The results from Wize Sniffer 1.0 correspondent to exhaled ethanol concentrations are reported in Table 7.

	Ethanol concentration (ppmv)
SUBJ 1- PRE SUBJ 1 - POST beer	1.32ppm 17.63ppm
SUBJ 2- PRE SUBJ 2 - POST prosecco	4.08ppm 10.17ppm
SUBJ 3- PRE SUBJ 3 - POST wine	5.75ppm 25.27ppm

Table 7- Wize Sniffer results relative to exhaled ethanol concentrations.

The Wize Sniffer 1.0 was able to return reliable results on a quality level, but, as expected, there was not an overlapping with the numerical results output from gas chromatography. Nevertheless, this is understandable, considering the different resolutions of the two techniques.

Validations of results by means of piCO+ Smokerlyzer

piCO+ Smokerlyzer (shown in Fig.35) is a device manufactured by Bedfont and commercialized by COSMED s.r.l.. It is a breath carbon monoxide monitor intended for multi-patient use by healthcare professionals in smoking cessation programs, research and as an indicator of carbon monoxide poisoning in a healthcare environment. Breath carbon monoxide is measured in ppm.

Fig.35- piCO+ Smokerlyzer is a device manufactured by Bedfont and commercialized by COSMED s.r.l.

Three subjects were taken from the population described previously: a male subject (SUBJ1), light smoker, a female subject (SUBJ2), moderate smoker, a female (SUBJ3), heavy smoker. All of them were normal body type and belonging to the age range [30-40].

The three subjects, one by one, first made three whole breaths in the Wize Sniffer, and then 1 whole breath in the piCO+ Smokerlyzer.

The tests were repeated after the subjects smoked a cigarette.

The results are shown in Table 8. The device was able to return reliable results both on a quality level and numerically.

	Smoking habit	PRE-WS	PRE-piCO+	POST-WS	POST- piCO+
SUBJ 1	1-2 cig./day	4.3ppm	3ppm	11.42ppm	8ppm
SUBJ 2	4-5 cig./day	5.9ppm	7ppm	13.01ppm	11ppm
SUBJ 3	20 cig./day	9.12ppm	11ppm	20.7ppm	17ppm

Table 8- Smoking habit: validations of results by means of piCO+ Smokerlyzer.

In this case, an overlapping could be expected, considering that both the device (piCO+ Smokerlyzer and Wize Sniffer 1.0.) base their transduction principle on a gas sensor.

5.3 Discussion on the WS 1.0

In this report, we have described the design of the Wize Sniffer (WS) 1.0 during the first 15-month period of activity. Such device was able to return, on a quality level, reliable outputs in response to the several test conditions.

WS 1.0 is able to detect exhaled ethanol and discriminate among different alcoholic grades, giving outputs in line with them: the voltage output raised in line with the increase in alcoholic grade. Similarly, the device output is able to follow the trend in time of alcohol adsorption, (disposal): during the tests, the voltage output raised in line with the increase, in amount, of the same alcoholic drink, and decreased in time, when alcohol consumption stopped, following the alcohol disposal.

Reliable outputs have been registered also during the test regarding smoking habit: the device is able to distinguish between smoker subjects and non-smoker subjects, as well as there was a rise in carbon monoxide and ammonia concentration values after smoking.

Interesting results were collected also during the test regarding carbohydrates metabolism: still on a quality level, hydrogen concentration values are in line with bibliography, showing an increase in case of subjects suffering overweight problems or after smoking, and a decrease in case of exercise or after drinking alcohol.

Concerning numerical results, that is, exhaled substances concentration numerical values, some considerations have to be made. The observed concentration values corresponding to exhaled ethanol were generally in line with the ones output from alcohol tester, even though we cannot conclude that there was a complete overlapping; on the contrast, no relevant overlapping has been observed when comparing with the results output from gas chromatography.

Nevertheless, this is reasonable considering the different resolutions of the several instrumentation. Gas cromatography-mass spectrometry is the gold-standard for gas analysis, having very high resolution and sensitivity. Gas chromatography is able to discriminate among several substances, one by one, with high precision and high resolution. On the other hand, our device is affected by sensors' cross-sensitivity: the presence of two multi-sensing sensor is an aspect that has not to be overlooked. If having multi-sensing sensors may be advantageous on one hand, because it allows to detect a wider set of analytes, on the other hand it affects the selectivity of the sensors themselves.

Furthermore, a strong hypothesis has been made in the model consisting five non-linear equations system to calculate exhaled molecules concentrations: for two multi-sensing sensors, we made the hypothesis that the several contributions from the several substances add together linearly. This is an aspect to be improved in the next future.

The comparison between the results obtained with the Wize Sniffer and the ones output from piCO+ Smokerlyzer has been rather satisfying. A relevant overlapping between the two different devices has been observed, due to the specific transduction function of both the systems.

6. THE SECOND WS: WIZE SNIFFER 1.1

During the performance tests, we noticed that one of the material used for the manufacture of the WS 1.1's storage chamber, containing Toluene, Isobutane can make the sensors saturate. As a consequence, in collaboration with COSMED, we retained worthwhile to realize a new storage chamber without using those materials which the sensors are sensitive to; in particular, COSMED realized the **Wize Sniffer 1.1** using **Delrin and ABS** for the storage chamber.
In addition, COSMED integrated a **fluximeter**, placed between the HME filter and the corrugated tube, in order to measure the volume of exhaled air by the subject (Figure 36).

Fig.36. Components improving the WS 1.1

Further efforts were made in order to:

- integrate the fluximeter in the circuit board;
- upgrade the code on Arduino IDE according to the functioning of the fluximeter;
- upgrade the Matlab code;

In particular, the circuit platform was adjusted as in Fig. 37. Platform dimensions were adjusted to make easier the seat of the platform itself in the device's case.
In the Wize Sniffer 1.1 another type of Arduino board will be used: Arduino Mega 2560. The choice was made because of its higher number of analogue pins (and avoid the use of multiplexer) and its SRAM, which is bigger than the one of Arduino Ethernet, used in WS 1.0 (8KByte vs 2Kbyte).
This allowed us to buffer the data streaming from the sensors in Arduino's SRAM and transmit them (again using a tcp/ip protocol) when available. Obviously, an Ethernet module (compatible with Arduino Mega 2560) is used.
The load resistors Rl for TGS2620 and TGS2602 were decreased from 15KOm to 1,2 KOhm in order to decrease the sensors baseline value.

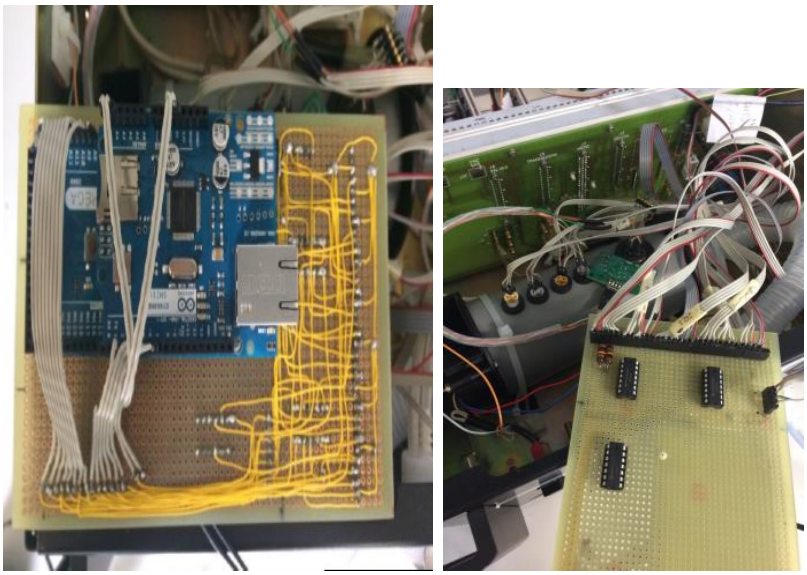

Fig.37 - The Arduino board with new circuit for the WS 1.1

Based on the previous considerations, the program implemented on Arduino was upgraded; a code for fluximeter's data reading and for data buffering was integrated. The data are transmitted from the Telnet Server only when the fluximeter starts to sense an air flow (i.e., when the user is blowing in the Wize Sniffer).
According to the Expiratory Table supplied by COSMED the expiratory volume is calculated using a Matlab routine.

Future Perspectives of the Wize Sniffer
In the immediate future, our efforts will be focused on the evaluation of the performances of the new Wize Sniffer 1.1 by means of (i) further tests; (ii) on the analysis of outcomes, by means of PCA, KNN algorithms etc.; (iii) on the implementation of a code in C necessary when the Wize Sniffer will be integrated in the Wize Mirror.

7. THE GAS SENSORS CUSTOMIZED WITH ELECTROSPUN NANOFIBERS

A preliminary research activity aimed at the optimization of the electrospinning conditions for the preparation of nanofibers based on an electrically conducting polymer was carried out. Polyaniline emeraldine base (PANi) doped with 10-camphorsulfonic acid (CSA) in the form of nanosized diameter fibers was selected as sensing material to improve sensor sensitivity and response time. PANi is one of the most investigated electrically conductive polymers for sensing materials development due its low cost, good ease of synthesis, environmental stability, adequate level of electrical conductivity, and wide range of technological applications[13]. However, the viscoelastic properties of PANisolutions in organic solvents are not well suited for electrospinning due to the polymer rigid backbone related to PAni molecule high aromacity as well as to its relatively low molecular weight [14]. Blending with polyethylene oxide (PEO), a more flexible polymer with better solubility and higher molecular weight, was investigated as means to improve PAni processing properties. Different experimental parameters, such as PAni/PEO ratio in the starting solution and electric field parameters, were investigated in order to optimize the nanofibers preparation process and the morphology of the collected nanofibrous meshes.

Materials

Polyaniline emeraldine base (PANi, Mw = 65,000), 10-camphorsulfonic acid (CSA), polyethylene oxide (PEO, Mw = 100,000) and chloroform (CHCl3, 99.8%) were purchased from Sigma-Aldrich (Italy) and used without further purification.

Methods

PANi solutions were prepared by dissolving at room temperature 120 mg of PANi in 6 mL of CHCl3 (2% w/v) under stirring for 4 h. 154 mg of CSA (0.5 molar ratio of CSA per repeat unit of PANi) were then added to the solution that was left under magnetic stirring at room temperature for 16h. The solution was filtered using a 0.2 µm PTFE filter (Millipore, Italy) to obtain a homogeneous mixture, and the desired amount of PEO was added followed by magnetic stirring at room temperature for 3 h.

The polymeric solution was loaded into a 10 mlsyringe fitted with a 21-gauge blunt tip stainless steel needle, and the solution feed rate was controlled by a syringe pump (BSP-99 M, Braintree Scientific Inc., Braintree, MA). An electric field was created between the tip of the needle and an aluminum screen by employing two high voltage power supplies of opposite polarity (Spellman High Voltage, UK) (Fig. 38).

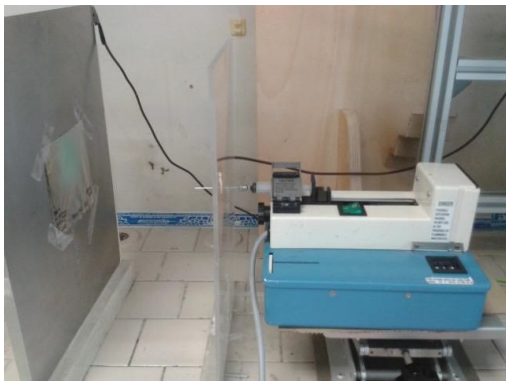

Fig. 38: Electrospinning set up comprising a syringe fitted with a blunt tip needle and a metallic screen as fibers collector

To determine the optimal electrical field parameters for electrospinning jet stability, various combinations between applied voltage (V) and needle tip to collector distance (d) were investigated varying V in the

range of 10–50 kV and d from 10 to 40 cm. The solution feed rate was varied between 0.1 and 5 mL/h. The processing time was 5 min for preliminary evaluations. All the fabricated meshes were first dried under a fume hood and then kept under vacuum for 24 h.
The morphology of electrospun samples was investigated by means of scanning electron microscopy (SEM; Jeol LSM 5600LV, Japan).

Results
The electrospinning conditions for the obtainment of PAni/PEO blend nanofibers were investigated by varying the ratio between the two polymers, employing different electric field parameters, and varying the solution feed rate (F).
When a PAni:PEO weight ratio of 1:1 was employed, an electrospinning jet was not ejected from the needle tip. However, when solutions containing a PAni/PEO weight ratio of 1:2 were processed a stable jet was achieved by applying a needle tip-collector distance (d) of 10 cm, a voltage (V) of 15 kV and a flow rate of 0.5 mL/h. SEM analysis of the obtained samples revealed highly porous mats composed of randomly oriented fibers with a diameter on the nanometer scale (Fig. 39).

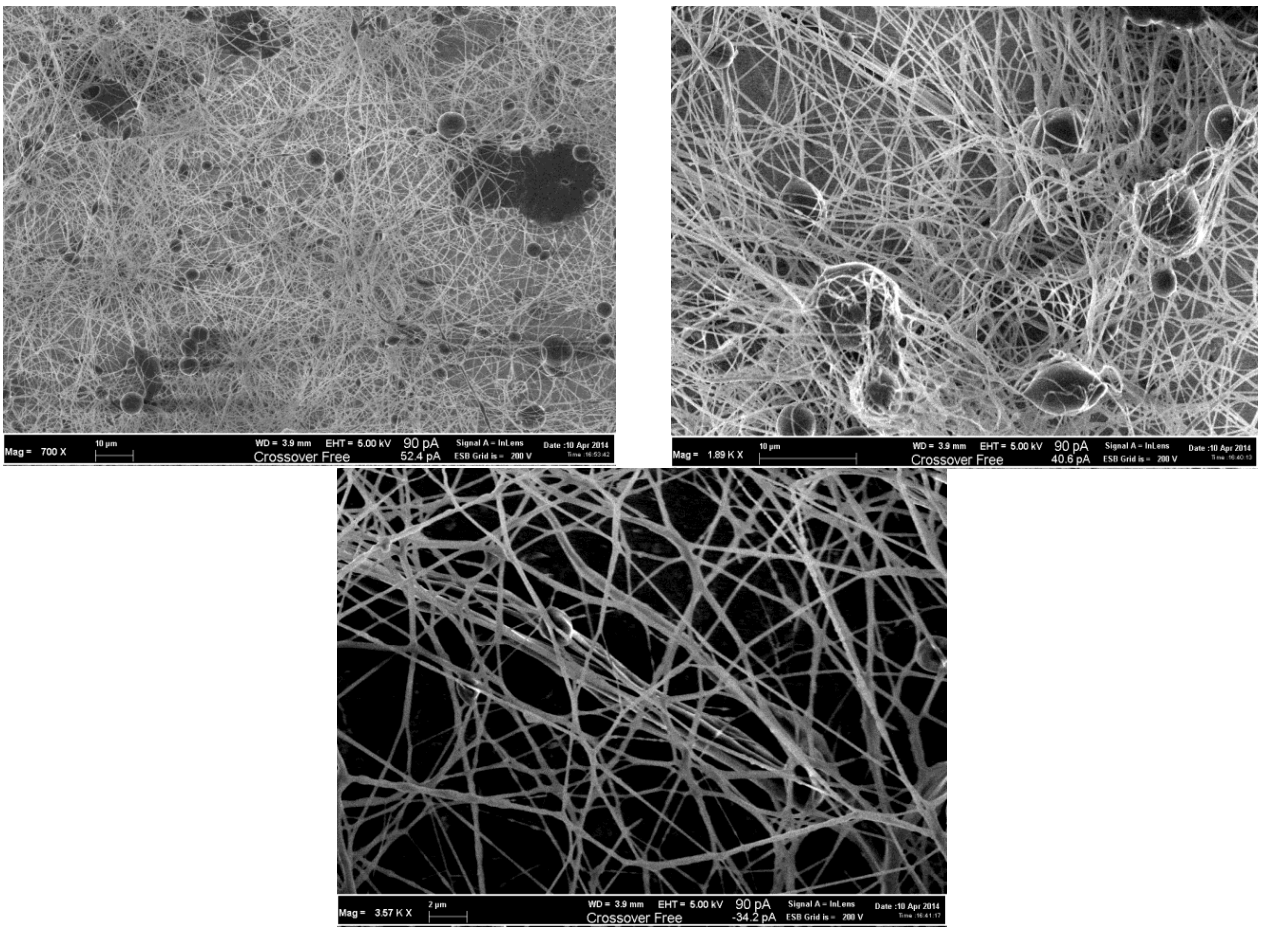

Fig. 39: Representative SEM micrographs at different magnifications of PAni/PEO electrospun mats

To obtain focused fibers collections, we tested a screen-to screen electrode configuration composed of two parallel metallic screens at different electrical potentials, one functioning as a fiber collector and the other one as an auxiliary electrode (Fig.41). This geometry is similar to that of a capacitor and allows the production of focused fiber collections by minimizing the area where the fibers are deposited [15-16]. The fluid was fed at a given flow rate to the metallic needle jutting out of a hole in the middle of one plate and the fibers were collected onto the other plate. To optimize the electric field strength various voltages, ranging from 15 to 40 kV, were applied to the two screens and different set of distances between the needle tip and the collector (d_1) and between the two screens (d_2) were employed.

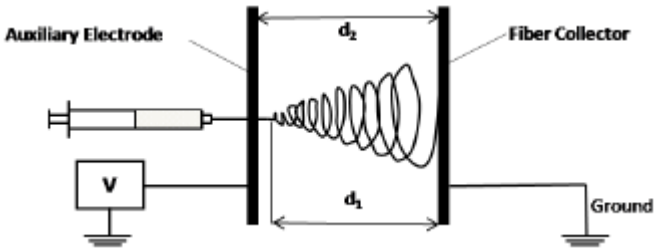

Fig. 40: Schematic representation of an electrospinning set up with Screen-to-Screen (StS) electrode configuration.

After a preliminary investigation, the optimal difference between d_1 and d_2 to obtain a stable polymeric solution jet was found to be 3cm. In addition, the critical d_1 for the achievement of a fibrous morphology was found to be 15cm. When a lower d_1 was applied, the fibrous morphology was partially compromised (Fig. 41) likely because of the residual solvent present in the collected fibers. Indeed, previous studies have shown that short needle tip-collector distances don't allow the fibers sufficient time to dry before reaching the collector [17].

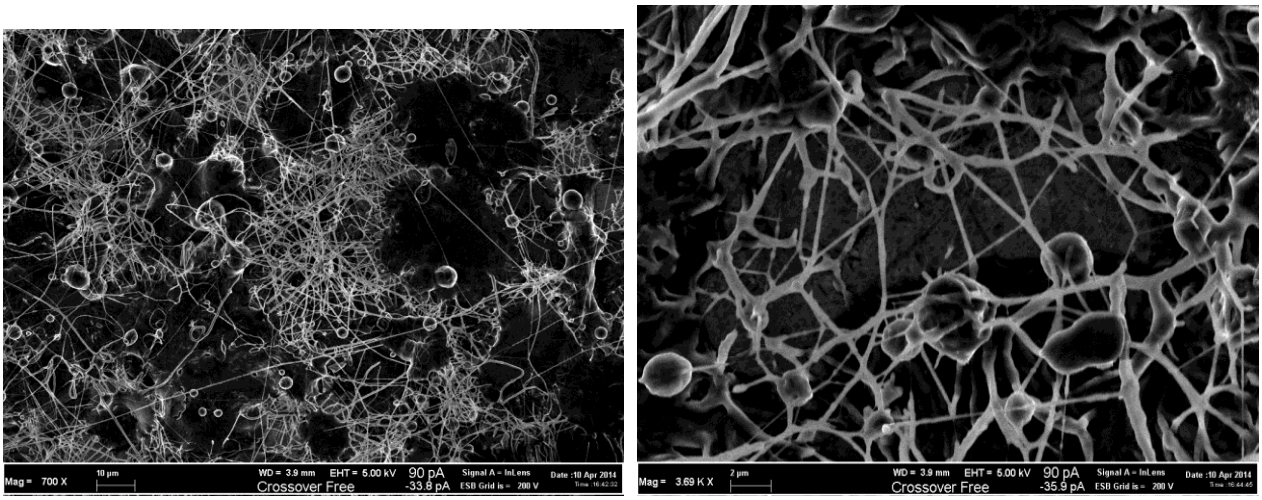

Fig. 41: Representative SEM micrographs at different magnifications of PAni/PEO electrospun mats produced by means of StS configuration. Electrospinning parameters: d1 = 10 cm, d2 = 13 cm, V = 15 kV, F = 1 ml/h.

Three-dimensional porous meshes with a non-woven nanofibrous structure were produced employing d_1 = 15, d_2 = 18 cm and V = 25 kV. However, when F = 1 ml/h was employed the fibrous morphology was characterized by a relatively high density of defects in the form of beads or beaded fibers (Figure 42). Nevertheless, a decrease of density of beads and other fiber defects was observed by decreasing F from 1 to 0.5 ml/h (Figure 43).

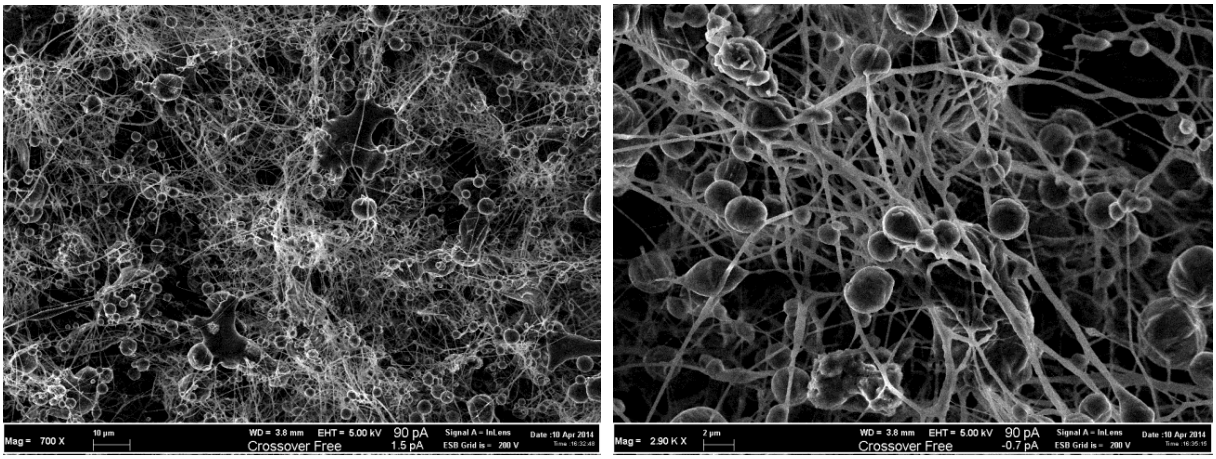

Fig.42: Representative SEM micrographs at different magnifications of PAni/PEO electrospun mats produced by means of StS configuration. Electrospinning parameters: d1 = 15 cm, d2 = 18 cm, V = 25 kV, F = 1 ml/h.

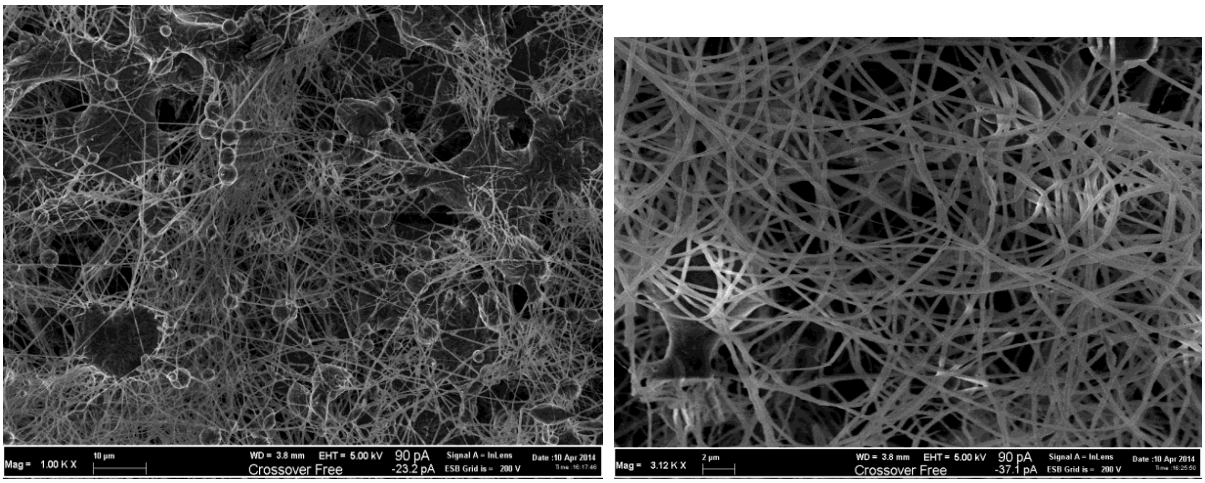

Fig.43: Representative SEM micrographs at different magnifications of PAni/PEO electrospun mats produced by means of StS configuration. Electrospinning parameters: d1 = 15 cm, d2 = 18 cm, V = 25 kV, F = 0.5 ml/h.

During the electrospinning process, the stability of the fluid jet is determined by a mass balance between the delivery rate of the solution jet to the capillary tip and the rate at which the solution is removed from the tip by the electric forces. By increasing the feeding rate, more solution is ejected from the tip of the needle in a given time; therefore, if the electric force is able to stretch the jet sufficiently, the resulting fibers will have larger diameters, otherwise beads are formed because of surface tension [18]. The results of our work are consistent with those of other studies reporting lower beads dimension and density by decreasing solution feed rate [19-20].

Conclusion and Future Perspectives for the development of nanofiber based sensors inside SEMEOTICONS

The experimental conditions for the preparation of electrospun PANi-based nanofibers were investigated achieving a good control over fibers collection morphology by acting on processing parameters such as solution composition and electric field parameters. Future activities will be focused on the assessment of the electrical conductivity of the developed nanofibers, the development of electrospinning conditions for collecting PANi-based nanofibers directly onto the electrodes sensors, and the effect of the nanofibrous coating on WS device performance.

8. REFERENCES

[1] World Health Organization. The Global Burden of Disease: 2004 and update 2008.

[2] Lison M. W.; Carl H.; Rafael P.; Dan L.; David N.; Mant D., Glasziou P., 2010. *What are the basic self-monitoring components for cardiovascular risk management?*, MC Medical Research Methodology, 10:105.

[3] Guo D.; Zhang D.; Li N.; Zhang L.; Yang J., 2007. *A Novel Breath Analysis System Based on Electronic Olfaction*, IEEE Transaction on Biomedical Engineering.

[4] Miekisch W.; Schubert J.; Nöeldge-Schomburg, G., 2004. *Breath analysis in critically ill patients: potential and limitations*, Expert Review Molecular Diagnosys , 4, 619-629.

[5] Di Francesco F.; Fuoco R.; Trivella M.; Ceccarini A. 2005. *Breath Analysis: trends in techniques and clinical applications*, Micromechanical Journal, 79, 405-410.

[6] D'Amico, A.; Di Natale C.; Paolesse R.; Macagnano A.; Martinelli E.; Pennazza G.; Santonico M.; Bernabei M.; Roscioni C.; Galluccio G. et al., 2007. *Olfactory systems for medical applications*, Sensors & Actuators: B-Chemical, 130, 458-465.

[7] M. D'Acunto, A. Benassi, F. Chiellini, D. Germanese *et al.* Wize Sniffer: a new portable device designed for selective olfaction, SuperHeal Conference Proceedings, Angers, 4-6 March, 2014, pp. 577-582.

[8] Ding B.; Wang M.; Yu J.; Sun G., 2009. *Gas Sensors based on Electrospun Nanofibers*, Sensors , 9, 1609-1624.

[9] Chen D.; Lei S.; Chen Y., 2011. *A single Polyaniline Nanofiber Field Effect Transistor and Its Gas Sensing Mechanisms*, Sensors, 11, 6509-6516.

[10] Slater, J.; Watt, E.; Freeman, N.; May, I.; Weir, D., 1992. *Gas and vapor detection with poly(pyrrole) gas sensors.* Analyst, 117, 1265-1270.

[11] Slater, J.; Paynter, J.; Watt, E., 1993. *Multilayer conducting polymer gas sensor arrays for olfactory sensing*. Analyst, 118, 379-384.

[12] Savage, N.; Chwierogh, B.; Ginwalla, A.; Patton, B.; Akbar, S.; Dutta, P., 2001. *Composite n-p semiconducting titanium oxides as gas sensors*. Sens. Actuat. B-Chem, 79, 17-27.

[13] Jaymand, M., 2013. *Recent progress in chemical modification of polyaniline*. Prog. Polym. Sci. 38, 1287-1306.

[14] Yu, J. H., Fridrikh, S. V., Rutledge, G. C. , 2006. *The Role of Elasticity in the Formation of Electrospun Fibers*, Polymer , 47, 4789–4797.

[15] Puppi, D., Piras, A.M., Detta, N., Dinucci, D., Chiellini, F, 2010. *Poly (lactic-co-glycolic acid) electrospun fibrous meshes for the controlled release of retinoic.* Acta Biomater. 6, 1258-1268.

[16] Puppi, D., Detta, N., Piras, A.M., Chiellini, F., Clarke, D.A., Reilly, G.C., Chiellini, E., 2010. *Development of Electrospun Three-arm Star Poly (ε-caprolactone) Meshes for Tissue Engineering Applications*. Macromol. Biosci. 10, 887-897.

[17] Pham, Q.P., Sharma, U., Mikos, A.G., 2006. *Electrospinning of polymeric nanofibers for tissue engineering applications: a review*. Tissue Eng.; 12: 1197–1211.

[18] Puppi, D., Piras, A.M., Detta, N., Ylikauppila, H., Nikkola, L., Ashammakhi, N., Chiellini, F., Chiellini, E., 2011. *Poly (vinyl alcohol)-based electrospun meshes as potential candidate scaffolds in regenerative medicine*. J. Bioact. Compat. Polym. 26, 20-34.

[19] Zong , X., Kim, K., Fang, D., Ran, S., Hsiao, B.S., Chu, B., 2002. *Structure and process relationship of electrospun bioabsorbable nanofiber membranes*. Polymer 43, 4403–4412.

[20] Zong, X.H., Li, S., Chen, E., Garlick, B., Kim, K-S, Fang, D., et al., 2004. *Prevention of Postsurgery-induced abdominal adhesions by electrospun bioabsorbable nanofibrous poly(lactideco- glycolide)-based membranes*. Ann. Surg. 240, 910–915.

[21] D.G. Thompson, P. Bin_eld, A. De Belder, J. O'Brien, S. Warren, 1985 *Extra intestinal influences on exhaled breath hydrogen measurements during the investigation of gastrointestinal disease*, Gut